Deep learning for medical imaging

Olivier Colliot, PhD
Research Director at CNRS
Co-Head of the ARAMIS Lab – www.aramislab.fr
PRAIRIE – Paris Artificial Intelligence Research Institute

Maria Vakalopoulou, PhD
Assistant Professor at CentraleSupelec
Mathematics and Informatics (MICS)
Office: Bouygues Building Sb.132

Master 2 - MVA

Course website: http://www.aramislab.fr/teaching/DLMI-2019-2020/
Piazza (for registered students): https://piazza.com/centralesupelec/spring2020/mvadlmi/

Acknowledgements

- The lecture is partially base on material by:
  - Daniel Rueckert
  - Ben Glocker

Thank you!!

General

- Proposal Deadline is today! Submit your proposals soon! ;)
- Include questions that you may have in the mail!

Previous Lecture
Semantic Segmenation

Introduction

- Semantic Segmentation

- Idea #2: Image Segmentation using Fully Convolutional Layers
  - Design a network as a bunch of convolutional layers to make predictions for pixels all at once!

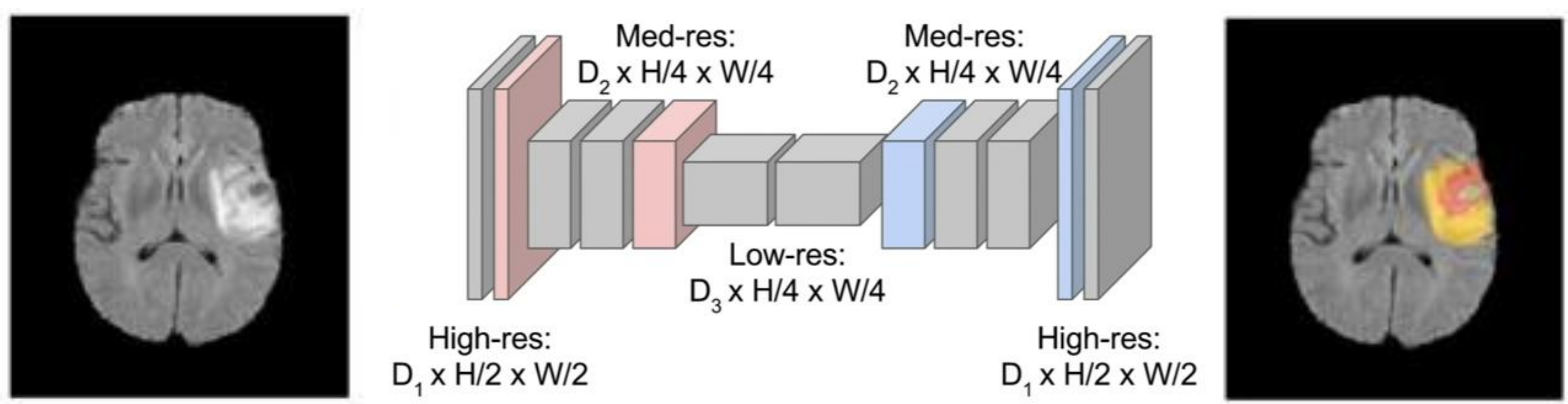

Input HxW

Output HxW

- Use Downsampling and upsampling inside the network!

Long, Shelhamer, and Darrell, "Fully Convolutional Networks for Semantic Segmentation", CVPR 2015
Noh et al, "Learning Deconvolution Network for Semantic Segmentation", ICCV 2015

Additional Losses

- **Dice Loss** [Milletari et al., 2016]

$$D = \frac{2\sum_i^N p_i g_i}{\sum_i^N p_i^2 + \sum_i^N g_i^2} \qquad \frac{\partial D}{\partial p_j} = 2\left[\frac{g_j\left(\sum_i^N p_i^2 + \sum_i^N g_i^2\right) - 2p_j\left(\sum_i^N p_i g_i\right)}{\left(\sum_i^N p_i^2 + \sum_i^N g_i^2\right)^2}\right]$$

g_n the value of segmentation at n and p_n the predicted probabilistic map

- **Generalized Dice Loss** [Sudre et al., 2017]

$$\mathrm{GDL} = 1 - 2\frac{\sum_{l=1}^2 w_l \sum_n r_{ln} p_{ln}}{\sum_{l=1}^2 w_l \sum_n r_{ln} + p_{ln}}, \qquad \frac{\partial \mathrm{GDL}}{\partial p_i} = -2\frac{(w_1^2 - w_2^2)\left[\sum_{n=1}^N p_n r_n - r_i \sum_{n=1}^N (p_n + r_n)\right] + N w_2 (w_1 + w_2)(1 - 2r_i)}{\left[(w_1 - w_2)\sum_{n=1}^N (p_n + r_n) + 2N w_2\right]^2}$$

r_n the value of segmentation at n, p_n the predicted probabilistic map, $w_l = 1/\Sigma(r_{ln})^2$

Used to deal with the correlation that exists between the size of the segment and the result of the dice!

Other Measures

Tana & Hanbury: "Metrics for evaluating 3D medical image segmentation: analysis, selection, and tool"

volume similarity

$$VS = 1 - \frac{\left||A| - |B|\right|}{|A| + |B|} = 1 - \frac{|FN - FP|}{2TP + FP + FN}$$

surface distance measures

- **Hausdorff distance**

$$HD = \max\big(h(A,B), h(B,A)\big)$$

$$h(A,B) = \max_{a \in A} \min_{b \in B} \|a - b\|$$

- **(symmetric) average surface distance**

$$ASD = \frac{d(A,B) + d(B,A)}{2}$$

$$d(A,B) = \frac{1}{N} \sum_{a \in A} \min_{b \in B} \|a - b\|$$

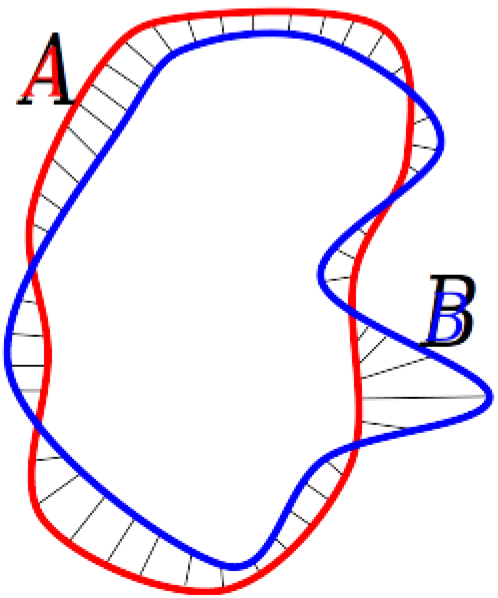

Part 5 – Denoising & Reconstruction

Outline

- Reconstruction
  - Problem statement
  - Traditional Methods
  - Recent Methods based on Deep Learning
- Denoising
- Recent Papers

MR image acquisition: Challenges

- Magnetic Resonance Imaging (MRI)
  - MRI acquisition is inherently a slow process
  - Slow acquisition is:
    - Ok for static objects (e.g. brain, bones etc)
    - Problematic for moving objects (e.g. heart, liver, fetus)
  - Options for MRI acquistion:
    - Real-time MRI: fast, but 2D and relatively poor image quality
    - Gated MRI: fine for period motion, e.g. respiration or cardiac motion but requires gating (ECG or navigators) leading to long acquisition times (30-90 min)

MR full acquisition

- MRI acquisition is performed in k-space by sequentially traversing sampling trajectories
  - One line by the time sequentially [physics limitations]
  - A simple linear operations using Fourier Transform to acquire the image

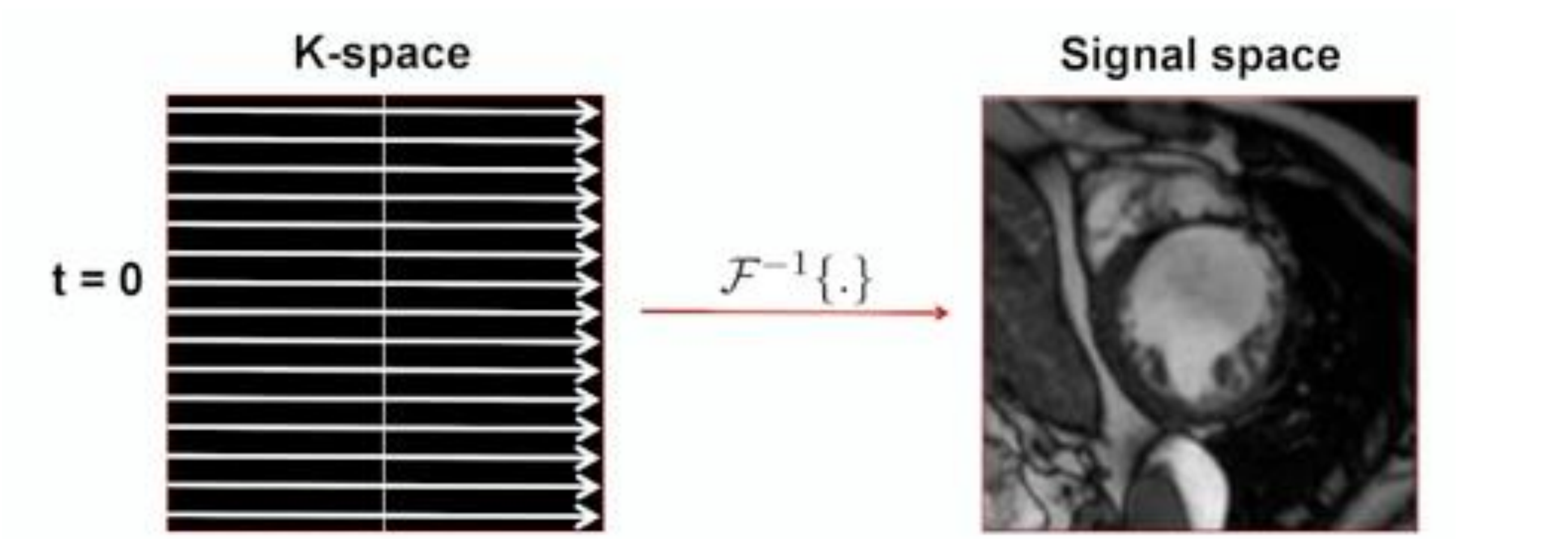

K-space undersampling

- Acquiring a fraction of k-space **accelerates** the process but introduces **aliasing/ smoothing** in signal space

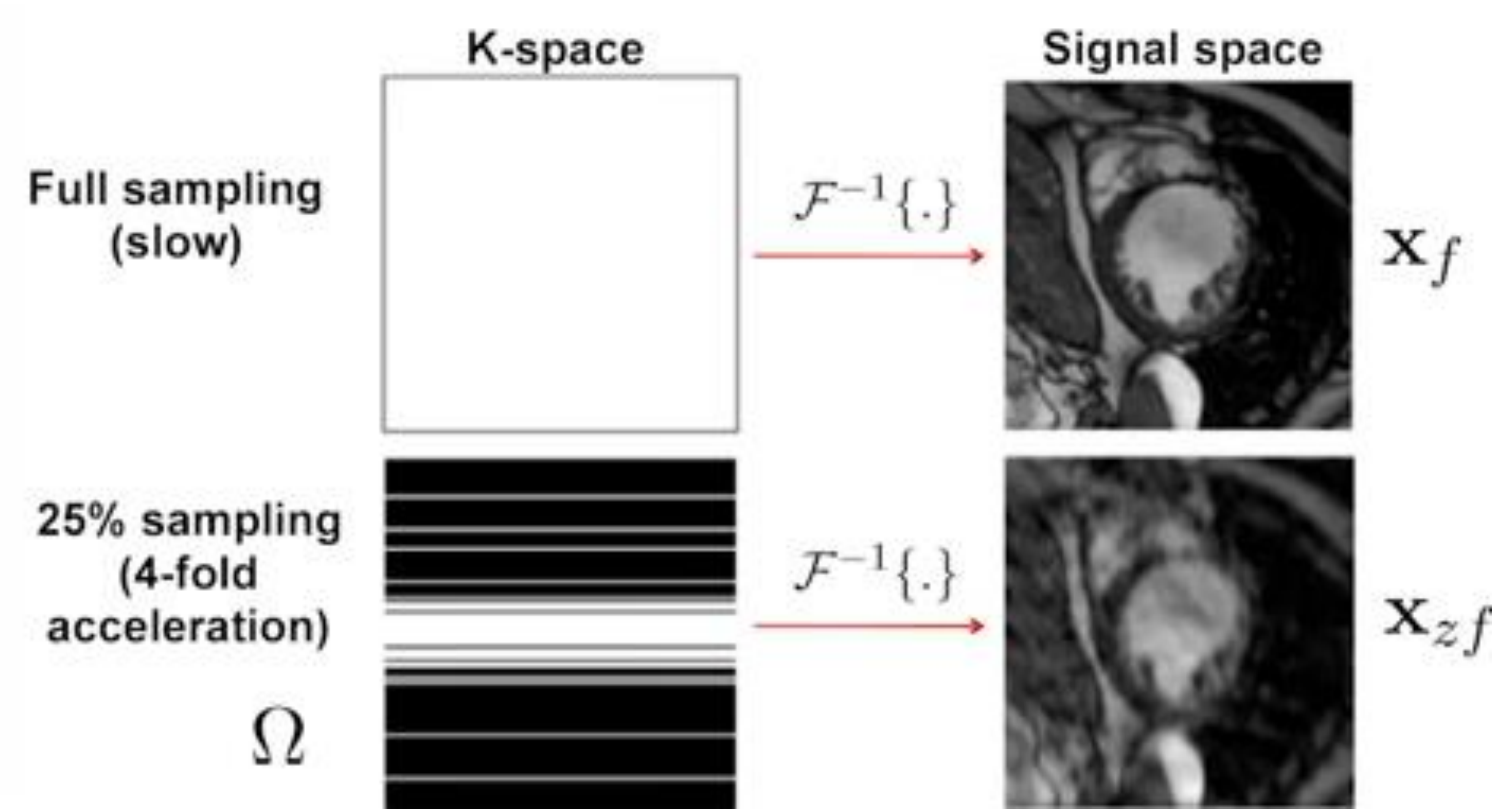

Introduction

- Image reconstruction from undersampled k-space an ill-posed inverse problem with undersample data
    - One can recover full k-space through compressed sensing techniques *[Based on generic priors e.g. sparsity or low rank]:*
        - Lusting et al., MRM 2007
        - Jung et al., MRM 2009
        - Otazo et al., MRM 2010

Introduction

- Image reconstruction from undersampled k-space an ill-posed inverse problem with undersample data
  - One can recover full k-space through compressed sensing techniques *[Based on generic priors e.g. sparsity or low rank]:*
    - Lusting et al., MRM 2007
    - Jung et al., MRM 2009
    - Otazo et al., MRM 2010
  - More recently other techniques have shown to be powerful for this task as well *[Based on learnt priors]*:
    - Caballero et al., IEEE TMI 2014: Dictionary learning
    - Bhatia et al., MICCAI2016: Manifold learning
    - Schlemper et al., IEEE TMI 2017: Deep Learning for cardiac MRI
    - K. Hammernik et al., MRM 2017: Deep learning for knee MRI

Sparsity

- Most natural signals are compressible under some domain

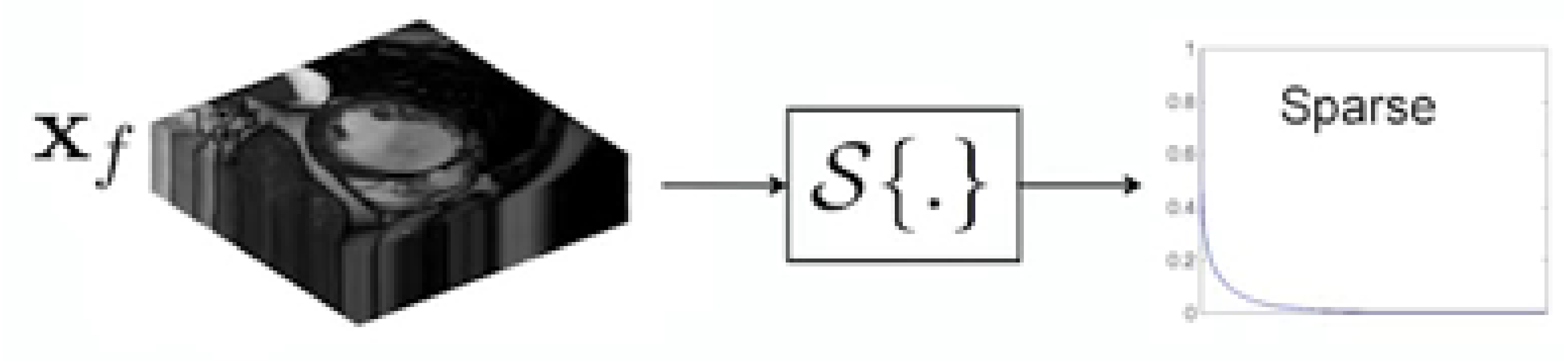

- Aliasing makes the assumption break down, so it can be imposed on the reconstruction of a signal

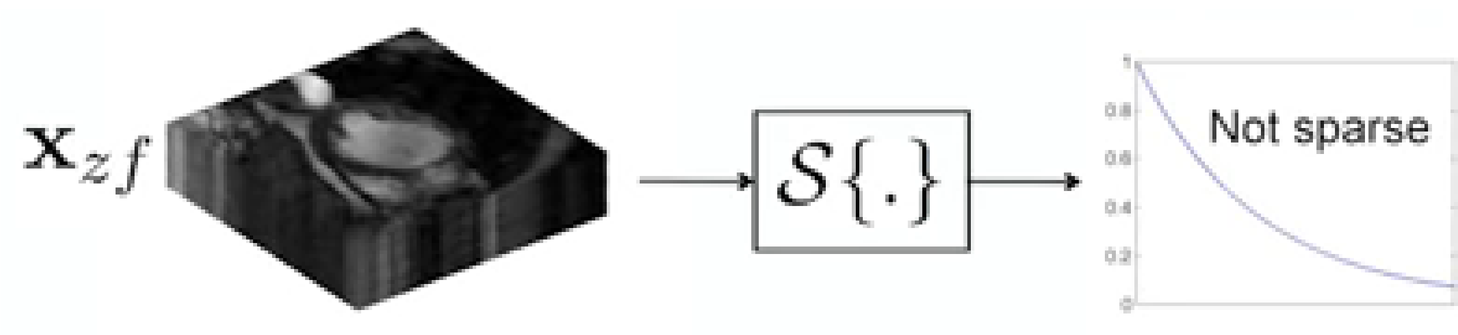

Compressed sensing

- Assume $\hat{\mathbf{x}}_u$ is the undersampled observation in k-space and $\mathcal{F}_u$ is the undersampled Fourier operator.
- We look for a solution $\mathbf{x}$ such that:
  - It is consistent with k-space observation

$$\boxed{\|\mathcal{F}_u\{\mathbf{x}\} - \hat{\mathbf{x}}_u\|_2^2 < \epsilon}$$

Compressed sensing

- Assume $\hat{\mathbf{x}}_u$ is the undersampled observation in k-space and $\mathcal{F}_u$ is the undersampled Fourier operator.
- We look for a solution $\mathbf{x}$ such that:
  - It is consistent with k-space observation
  - It has the sparsest representation under $\mathcal{S}\{\mathbf{x}\}$

$$\|\mathcal{F}_u\{\mathbf{x}\} - \hat{\mathbf{x}}_u\|_2^2 < \epsilon$$

$$\min_{\mathbf{x}} \|\mathcal{S}\{\mathbf{x}\}\|_0$$

Compressed sensing

- Assume $\hat{\mathbf{x}}_u$ is the undersampled observation in k-space and $\mathcal{F}_u$ is the undersampled Fourier operator.
- We look for a solution $\mathbf{x}$ such that:
  - It is consistent with k-spase observation
  - It has the sparsest representation under $\mathcal{S}\{\mathbf{x}\}$

Optimization problem:

$$\min_{\mathbf{x}} \|\mathcal{S}\{\mathbf{x}\}\|_0 \qquad s.t. \qquad \|\mathcal{F}_u\{\mathbf{x}\} - \hat{\mathbf{x}}_u\|_2^2 < \epsilon$$

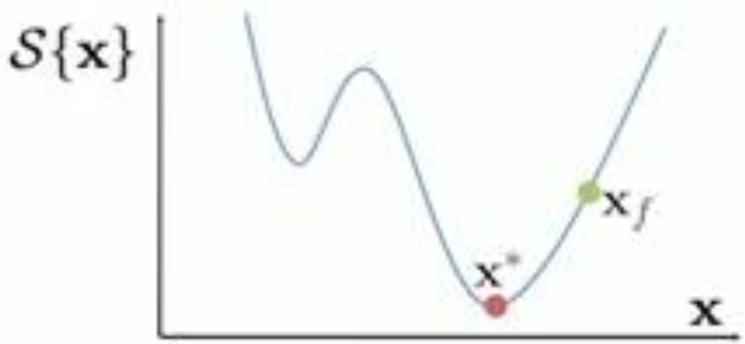

Need to ensure that transform $\mathcal{S}\{\mathbf{x}\}$ really does provide the sparsest representation in the solution space generated.

Dictionary learning for MR reconstruction

- Objective: Out of all solutions consistent with the acquired k-space, we look for the one that is sparsest under the learned dictionary

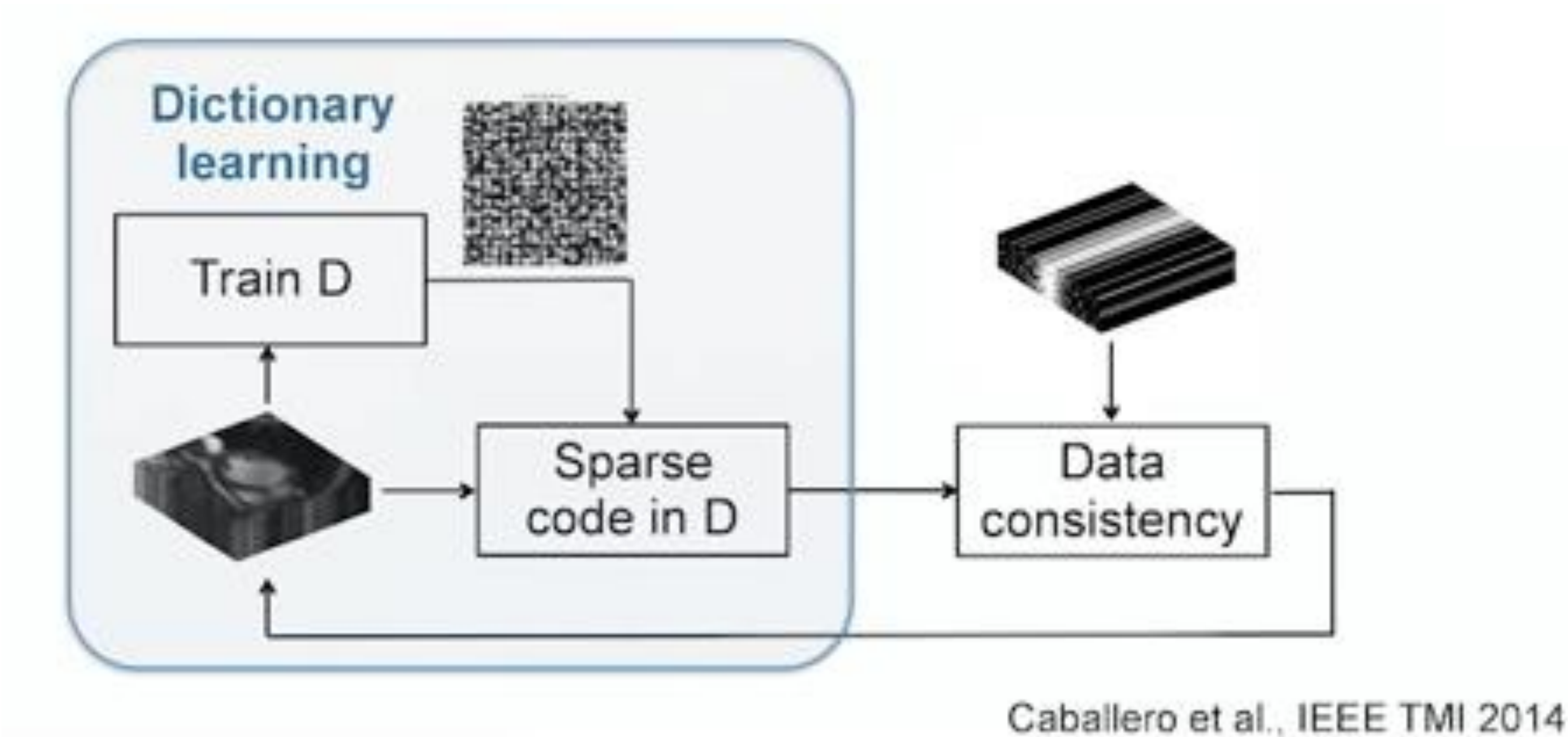

Dictionary learning for MR reconstruction

- Step 1: learn a dictionary that will sparsely represent 3D patches randomly extracted from the corrupted sequence

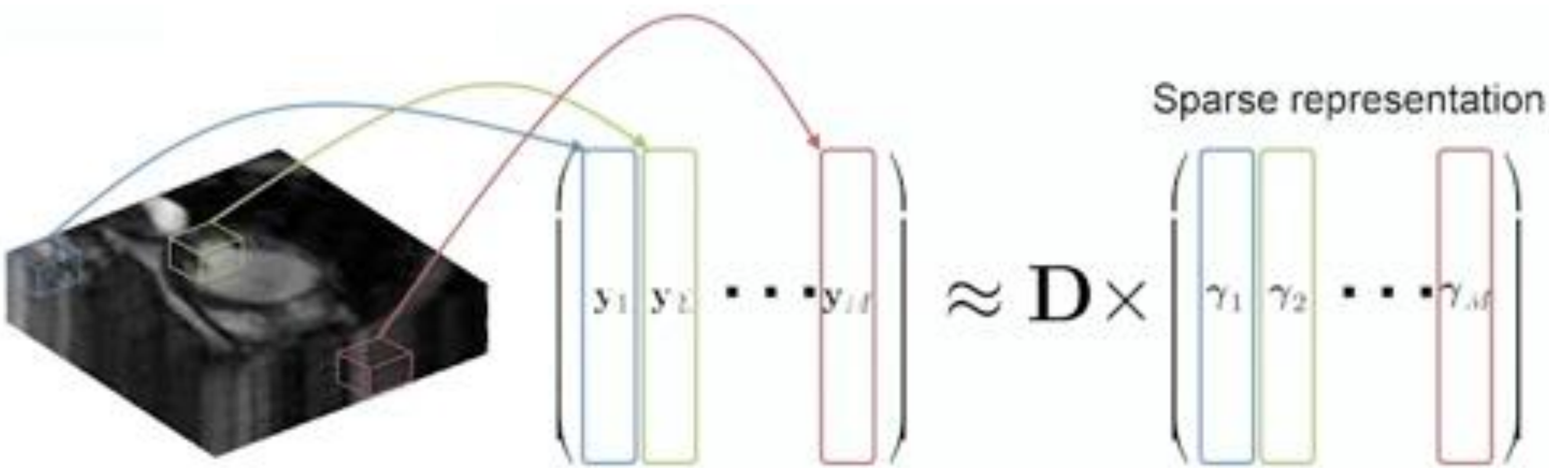

$$\min_{\boldsymbol{\Gamma},\mathbf{D}} \|\boldsymbol{\gamma}_i\|_0 \quad s.t. \quad \|\mathbf{y}_i - \mathbf{D}\boldsymbol{\gamma}_i\|_2^2 < \epsilon, \forall i$$

Dictionary learning for MR reconstruction

- The dictionary is adapted to features in the data and by construction provides a sparse represenation of it.
- Example for cardiac MRI

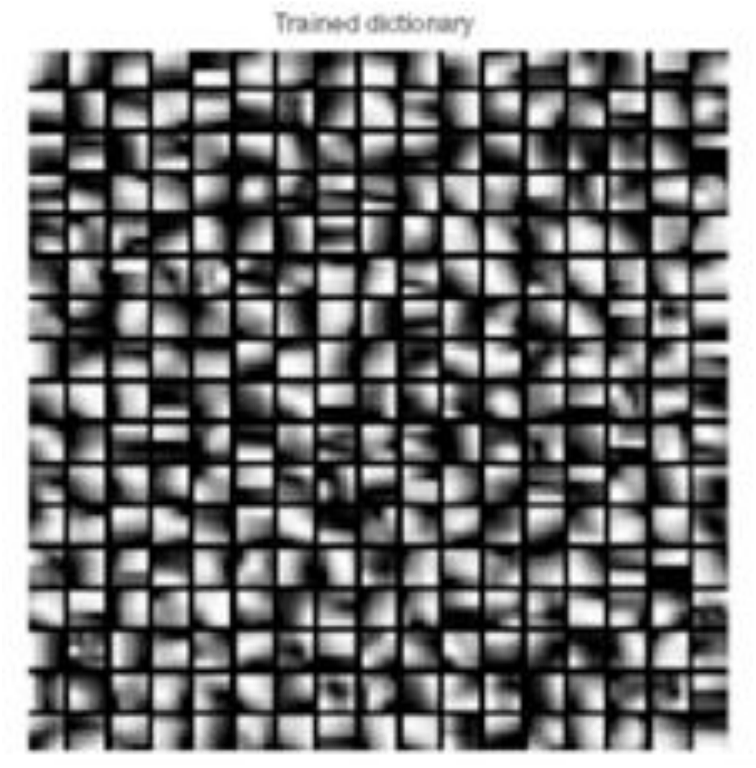

Dictionary learning for MR reconstruction

- Step 2: Sparse coding the entire sequence is sparsely coded using D.

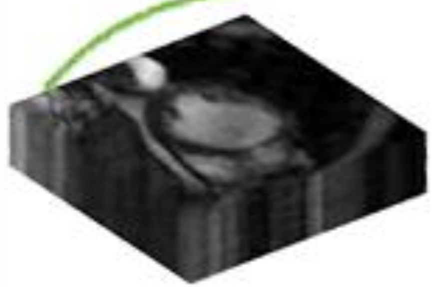

$$\min_{\boldsymbol{\Gamma}} \sum_{j=1}^{P} \|\boldsymbol{\gamma}_j\|_0 \quad s.t. \quad \sum_{j=1}^{P} \|\mathbf{R}_j\mathbf{y} - \mathbf{D}\boldsymbol{\gamma}_j\|_2^2 < \epsilon_1$$

- The sparse coding Γ provides an approximation of the sequence DΓ excluding part of the aliasing

$\boldsymbol{\Gamma}$: Sparse representation under $\mathbf{D}$

$\mathbf{D}\boldsymbol{\Gamma}$: Sparse approximation of $\mathbf{y}$

Dictionary learning for MR reconstruction

- Step 3: Data consistency
- Processing in signal space will make the k-space of solution x different from the initial observations
- Data consistency in k-space must be enforced.

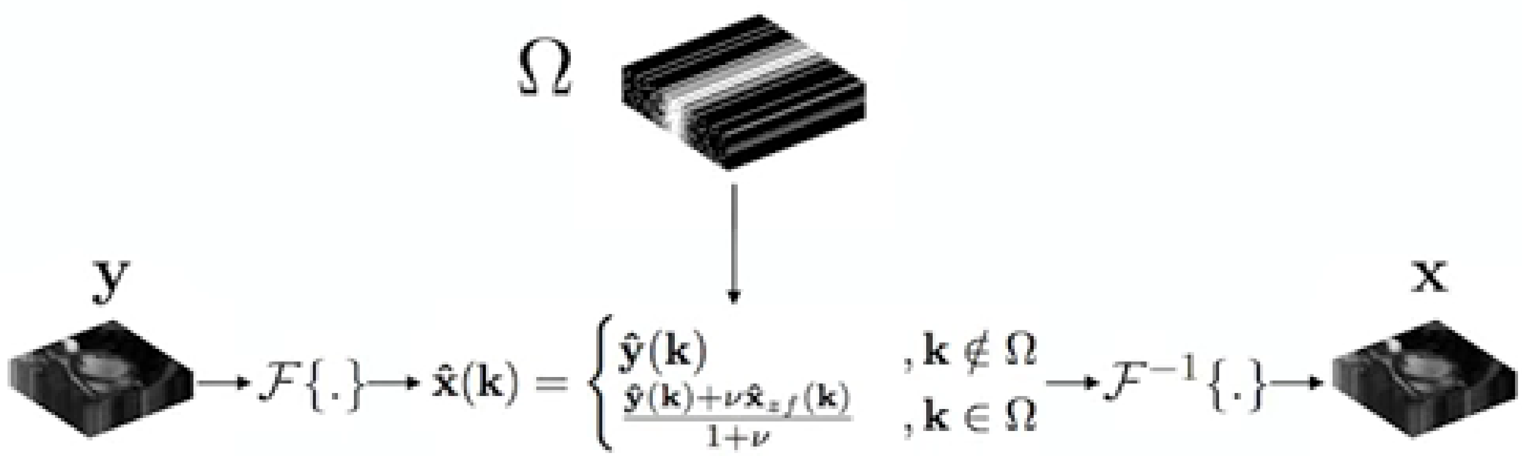

Problem formulation

- Reconstruct image $\mathbf{x} \in \mathbb{C}^n$ given undersampled k-space measurements $\mathbf{y} \in \mathbb{C}^M (M \ll N)$

$$\mathbf{y} = \mathbf{F}_u \mathbf{x} + \mathbf{e}$$

Undersampled Fourier encoding matrix

Acquisition noise

- In the case of Cartesian sampling we have $\mathbf{F}_u = \mathbf{M}\mathbf{F}$ where $\mathbf{F} \in \mathbb{C}^{\mathrm{N} \times \mathrm{N}}$ applies the 2D Fourrier transform and $\mathbf{M} \in \mathbb{C}^{M \times N}$ is the undersampling mask in k-space

Problem formulation

- We are trying to solve the following unconstrained optimisation problem:

$$\min_{x} \mathcal{R}(\mathbf{x}) + \lambda ||\mathbf{y} - \mathbf{F}_u \mathbf{x}||_2^2$$

Regularisation term (e.g. l_1)

Data Fidelity term

CNN-based solution

- Idea #1: Try to address the problem of denoising/ reconstruction as a semantic segmentation problem
  - Make use of the FCN architectures

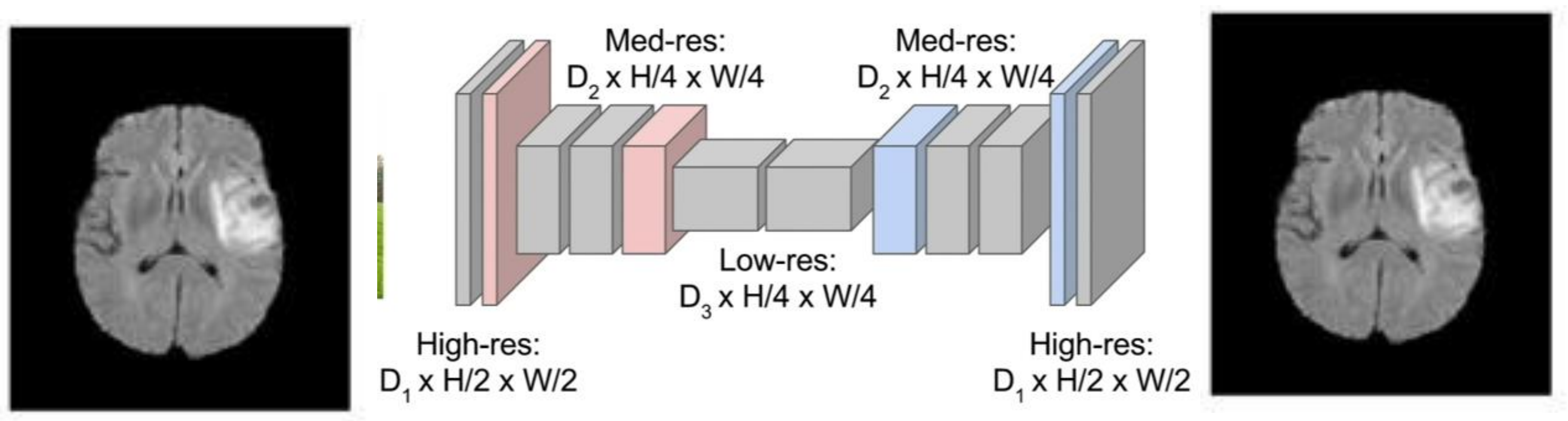

- Use Downsampling and upsampling inside the network!

Long, Shelhamer, and Darrell, "Fully Convolutional Networks for Semantic Segmentation", CVPR 2015
Noh et al, "Learning Deconvolution Network for Semantic Segmentation", ICCV 2015

Evaluation metrics

- For the quantitavie evaluation of the results some of the metrics used are:
  - Mean Square Error (MSE)

$$MSE = \frac{1}{m\,n}\sum_{i=0}^{m-1}\sum_{j=0}^{n-1}[I(i,j) - K(i,j)]^2$$

Evaluation metrics

- For the quantitavie evaluation of the results some of the metrics used are:
  - Mean Square Error (MSE)

$$MSE = \frac{1}{m\,n}\sum_{i=0}^{m-1}\sum_{j=0}^{n-1}[I(i,j) - K(i,j)]^2$$

  - Peak Signal to Noise Ration (PSNR)

$$\begin{aligned} PSNR &= 10 \cdot \log_{10}\left(\frac{MAX_I^2}{MSE}\right) \\ &= 20 \cdot \log_{10}\left(\frac{MAX_I}{\sqrt{MSE}}\right) \\ &= 20 \cdot \log_{10}(MAX_I) - 10 \cdot \log_{10}(MSE) \end{aligned}$$

MAX_I: Maximum possible pixel value of the image.

  - Structural Similarity Index (SSI)

$$SSIM(x,y) = l(x,y).\,c(x,y).\,s(x,y) = \frac{(2\mu_x\mu_y + c_1)(2\sigma_x\sigma_y + c_2)(cov_{xy} + c_3)}{(\mu_x^2 + \mu_y^2 + c_1)(\sigma_x^2 + \sigma_y^2 + c_2)(\sigma_x\sigma_y + c_3)}$$

$Conv_{xy}$: covariance of x and y; L the dynamic range of values; $k_1 = 0.01$, $k_2=0.03$

$$c_1 = (k_1 L)^2,\ c_2 = (k_2 L)^2 \text{ et } c_3 = \frac{c_2}{2}$$

Evaluation metrics

- For the quantitavie evaluation of the results some of the metrics used are:
  - Mean Square Error (MSE)

$$MSE = \frac{1}{m\,n}\sum_{i=0}^{m-1}\sum_{j=0}^{n-1}[I(i,j) - K(i,j)]^2$$

  - Peak Signal to Noise Ration (PSNR)

$$\begin{aligned} PSNR &= 10 \cdot \log_{10}\left(\frac{MAX_I^2}{MSE}\right) \\ &= 20 \cdot \log_{10}\left(\frac{MAX_I}{\sqrt{MSE}}\right) \\ &= 20 \cdot \log_{10}(MAX_I) - 10 \cdot \log_{10}(MSE) \end{aligned}$$

MAX_I: Maximum possible pixel value of the image.

  - Structural Similarity Index (SSI)
  - Signal to Noise Ration (SNR)
  - Edge Preservation Index (EPI)
  - Coefficient of Correlation (CoC)

Some Losses for Image Denoising

- [Zhao et al. 2017]
  - The l_1 error

$$\mathcal{L}^{\ell_1}(P) = \frac{1}{N} \sum_{p \in P} |x(p) - y(p)| \,, \qquad \partial \mathcal{L}^{\ell_1}(P) / \partial x(p) = \operatorname{sign}\left(x(p) - y(p)\right).$$

  - The l_2 error

Some Losses for Image Denoising

- [Zhao et al. 2017]
  - The l_1 error

$$\mathcal{L}^{\ell_1}(P) = \frac{1}{N}\sum_{p\in P} |x(p) - y(p)|, \qquad \partial\mathcal{L}^{\ell_1}(P)/\partial x(p) = \mathbf{sign}\left(x(p) - y(p)\right).$$

  - The l_2 error
  - The SSIM

$$\begin{aligned} \mathrm{SSIM}(p) &= \frac{2\mu_x\mu_y + C_1}{\mu_x^2 + \mu_y^2 + C_1} \cdot \frac{2\sigma_{xy} + C_2}{\sigma_x^2 + \sigma_y^2 + C_2} \\ &= l(p) \cdot cs(p) \end{aligned} \qquad \mathcal{L}^{\mathrm{SSIM}}(P) = \frac{1}{N}\sum_{p\in P} 1 - \mathrm{SSIM}(p).$$

$$\begin{aligned} &\frac{\partial\mathcal{L}^{\text{MS-SSIM}}(P)}{\partial x(q)} \\ &= \left(\frac{\partial l_M(\tilde{p})}{\partial x(q)} + l_M(\tilde{p}) \cdot \sum_{i=0}^{M} \frac{1}{cs_i(\tilde{p})} \frac{\partial cs_i(\tilde{p})}{\partial x(q)}\right) \cdot \prod_{j=1}^{M} cs_j(\tilde{p}), \end{aligned}$$

  - Adverarial Losses

DeepResolve

- [Chaudhari et al. 2017]: CNNs for super resolution for generating thin-slice MR images from thicker input slices.

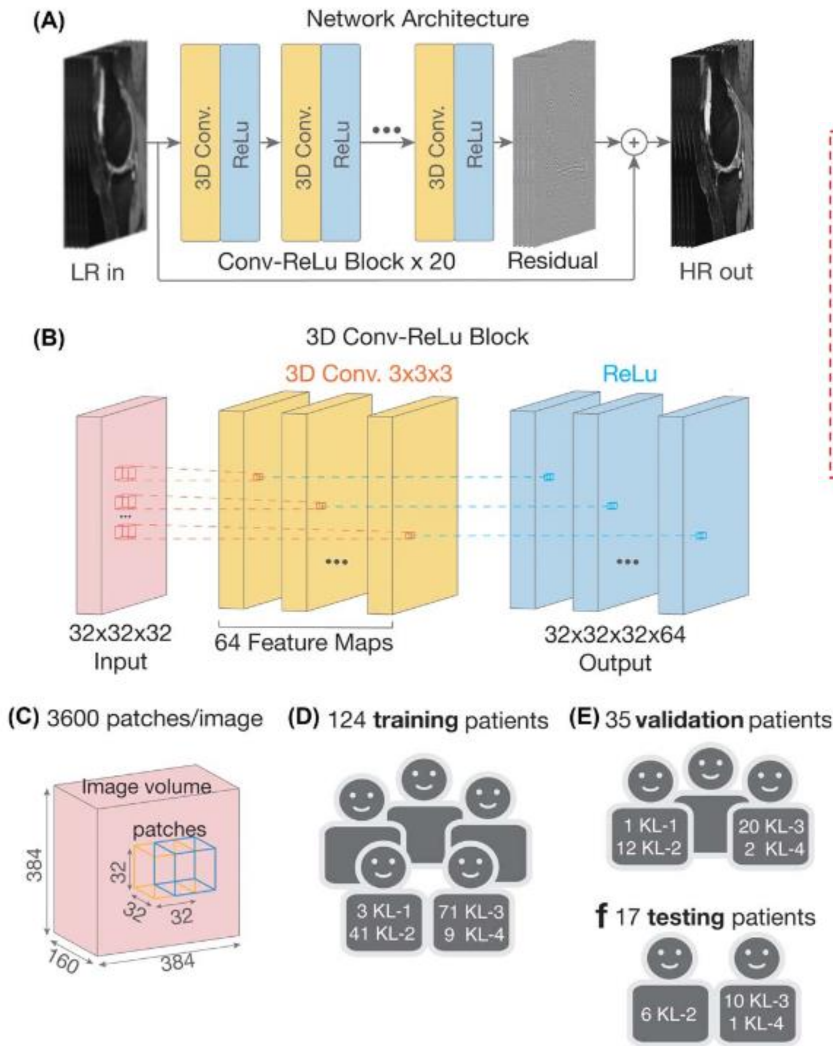

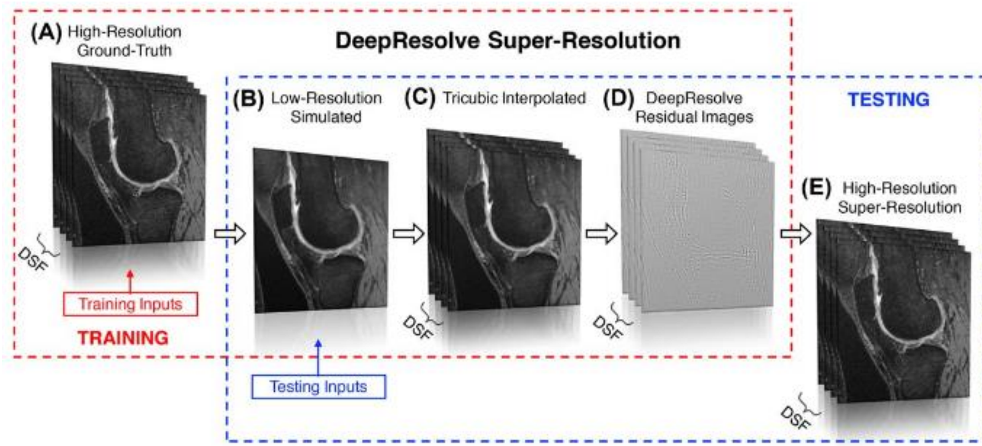

Use of l_2 loss

DeepResolve

- [Chaudhari et al. 2017]: CNNs for super resolution for generating thin-slice MR images from thicker input slices.

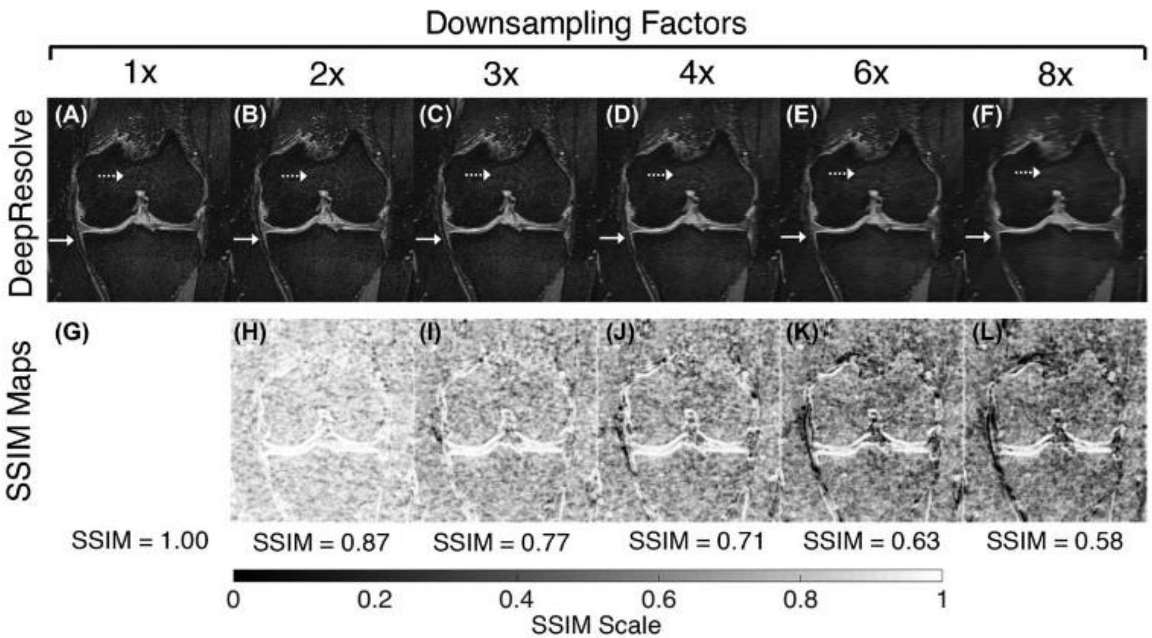

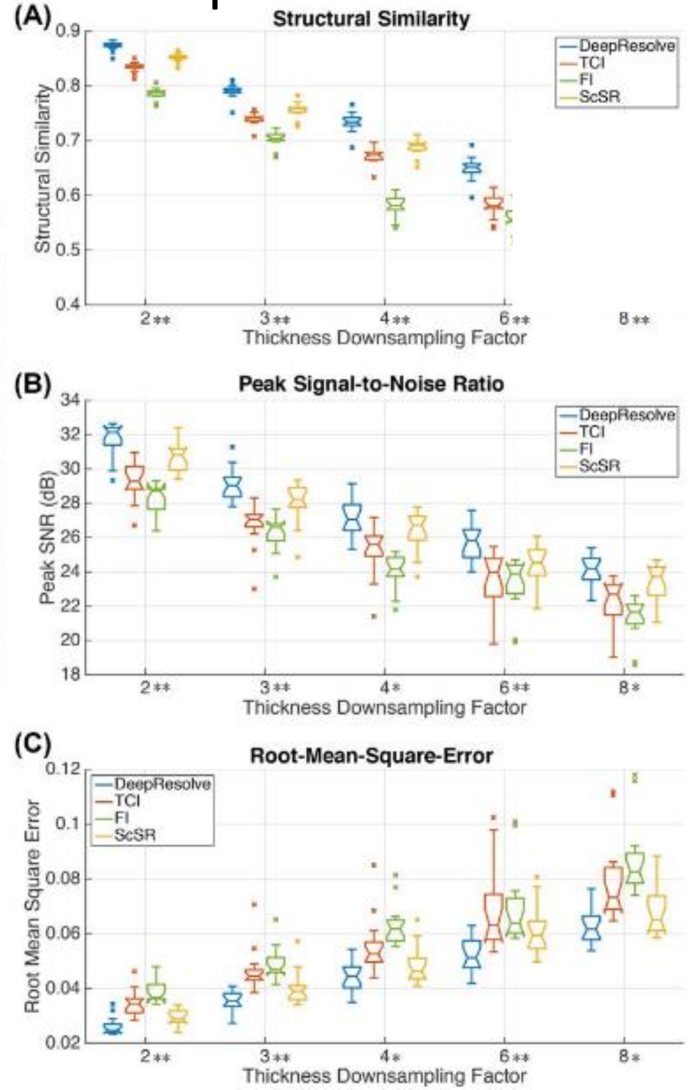

CNN-based solution

- Idea #2: Integrate the physics
- For CNN based reconstruction we formulate the problem as

$$\min_{x} ||\mathbf{x} - f_{cnn}(\mathbf{x}_u|\theta)||_2^2 + \lambda||\mathbf{F}_u\mathbf{x} - \mathbf{y}||_2^2$$

- Propose CNN modules that are more specific to the problem
- To ensure data fidelity, we add a data consistency layer. For fixed network parameters we can write:

$$\mathbf{s}_{rec} = \begin{cases} \mathbf{s}_{cnn}(j) & \text{if } j \notin \Omega \\ \frac{\mathbf{s}_{cnn}(j)+\lambda\mathbf{s}_0(j)}{1+\lambda} & \text{if } j \in \Omega \end{cases}$$

Data consistency layer

- To ensure data fidelity, we add a data consistency layer. For fixed network parameters we can write:

$$\mathbf{s}_{rec} = \begin{cases} \mathbf{s}_{cnn}(j) & \text{if } j \notin \Omega \\ \frac{\mathbf{s}_{cnn}(j) + \lambda \mathbf{s}_0(j)}{1+\lambda} & \text{if } j \in \Omega \end{cases}$$

Missing part of k-space

Acquired part of k-space

Fourier-encoding of reconstructed image

Zero-filled k-space

$$\mathbf{s}_{cnn} = \mathbf{F}\mathbf{x}_{cnn} = \mathbf{F} f_{cnn}(\mathbf{x}_u|\theta)$$

Data consistency layer

- End-to-end training requires specification of forward and backward passes
- Forward pass:

$$f_L(\mathbf{x}, \mathbf{y}; \lambda) = \mathbf{F}^H \mathbf{\Lambda} \mathbf{F} \mathbf{x} + \frac{\lambda}{1+\lambda} \mathbf{F}_u^H \mathbf{y}$$

Data consistency layer

- End-to-end training requires specification of forward and backward passes
- Forward pass:

$$f_L(\mathbf{x}, \mathbf{y}; \lambda) = \mathbf{F}^H \boldsymbol{\Lambda} \mathbf{F}\mathbf{x} + \frac{\lambda}{1+\lambda}\mathbf{F}_u^H \mathbf{y}$$

- Backward pass:

$$\frac{\partial f_L}{\partial \mathbf{x}^T} = \mathbf{F}^H \boldsymbol{\Lambda} \mathbf{F}$$

Jacobian of the DC layer with respect to the layer input x

$$\left[\frac{\partial f_{dc}(\mathbf{s}, \mathbf{s_0}; \lambda)}{\partial \lambda}\right] = \begin{cases} 0 & \text{if } j \notin \Omega \\ \frac{\mathbf{s}_0(j) - \mathbf{s}_{cnn}(j)}{(1+\lambda)^2} & \text{if } j \in \Omega \end{cases}$$

Derivatives with respect to the parameters λ

$$\boldsymbol{\Lambda}_{kk} = \begin{cases} 1 & \text{if } j \notin \Omega \\ \frac{1}{1+\lambda} & \text{if } j \in \Omega \end{cases}$$

Deep Cascade CNNs

- [Schlemper et al. 2017]: A convolutional architecture which takes into account the Fourier encoding

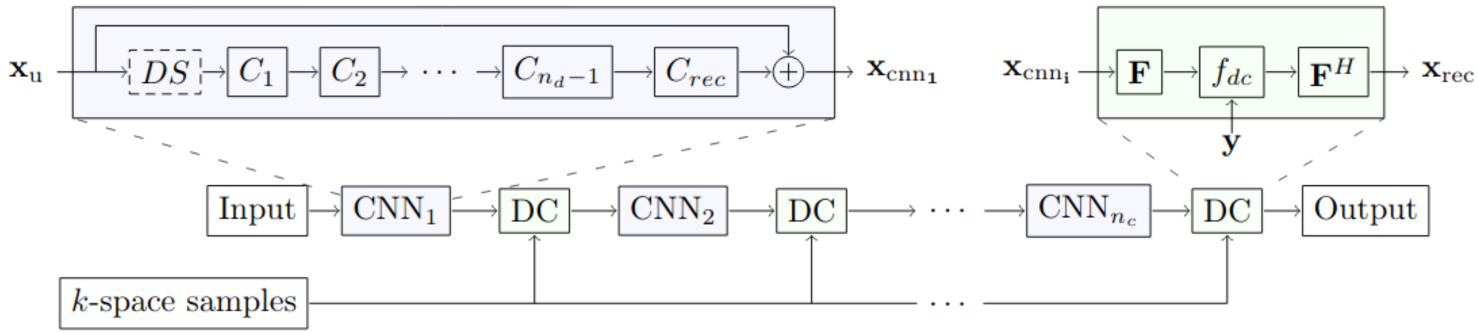

$$\mathbf{s}_{rec} = \begin{cases} \mathbf{s}_{cnn}(j) & \text{if } j \notin \Omega \\ \frac{\mathbf{s}_{cnn}(j) + \lambda \mathbf{s}_0(j)}{1+\lambda} & \text{if } j \in \Omega \end{cases}$$

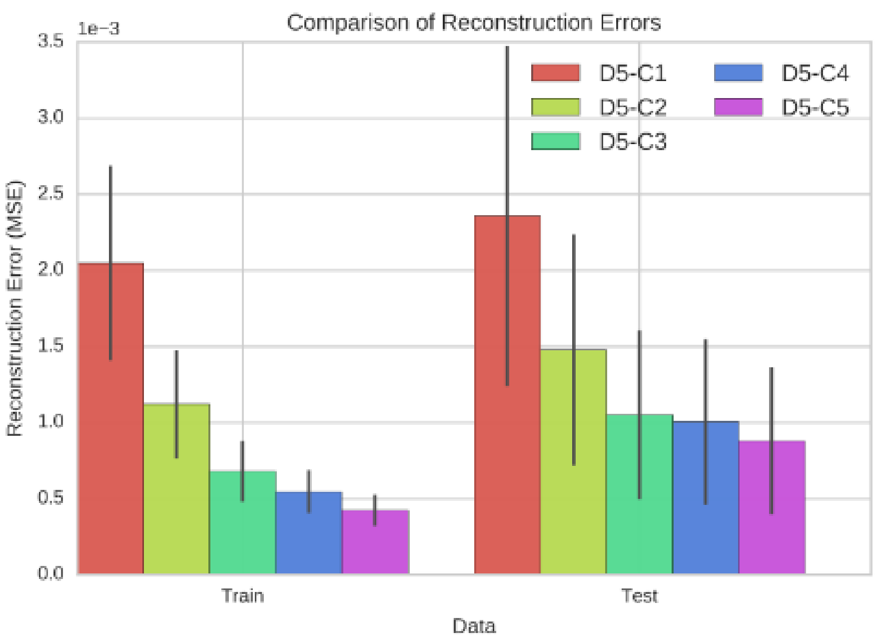

Deep Cascade CNNs

- [Schlemper et al. 2017]: Results

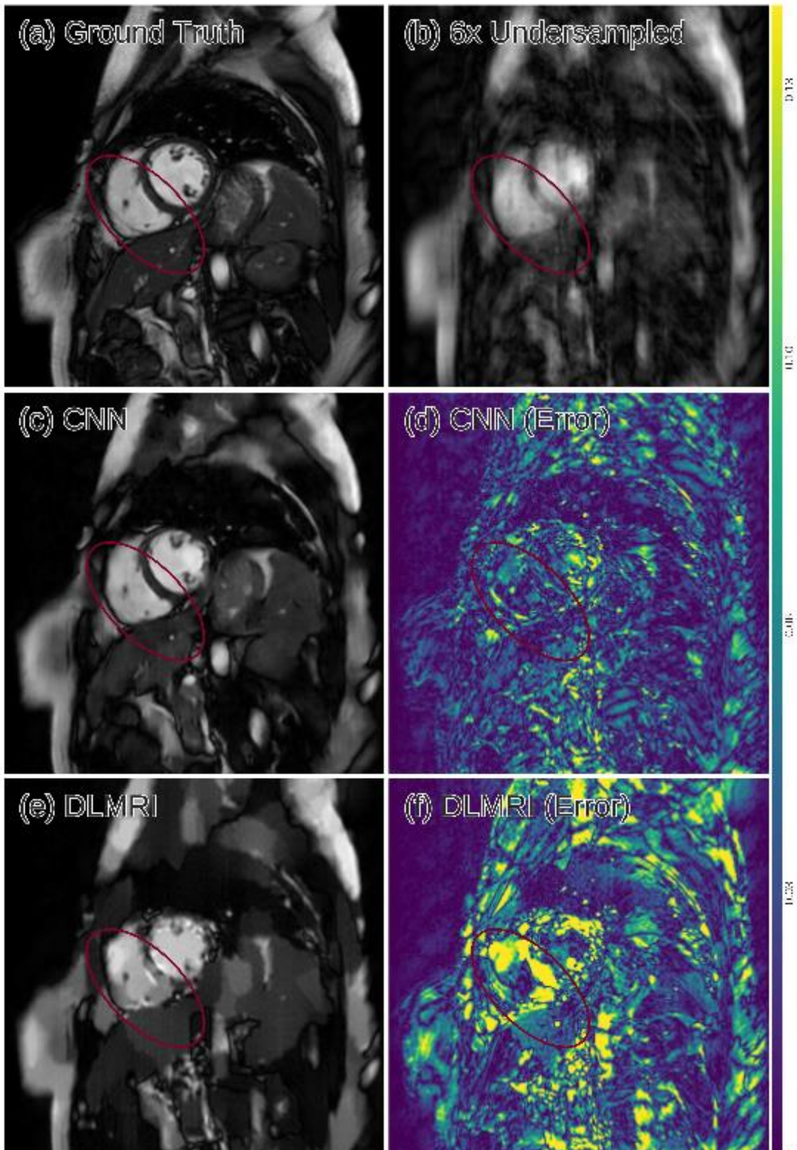

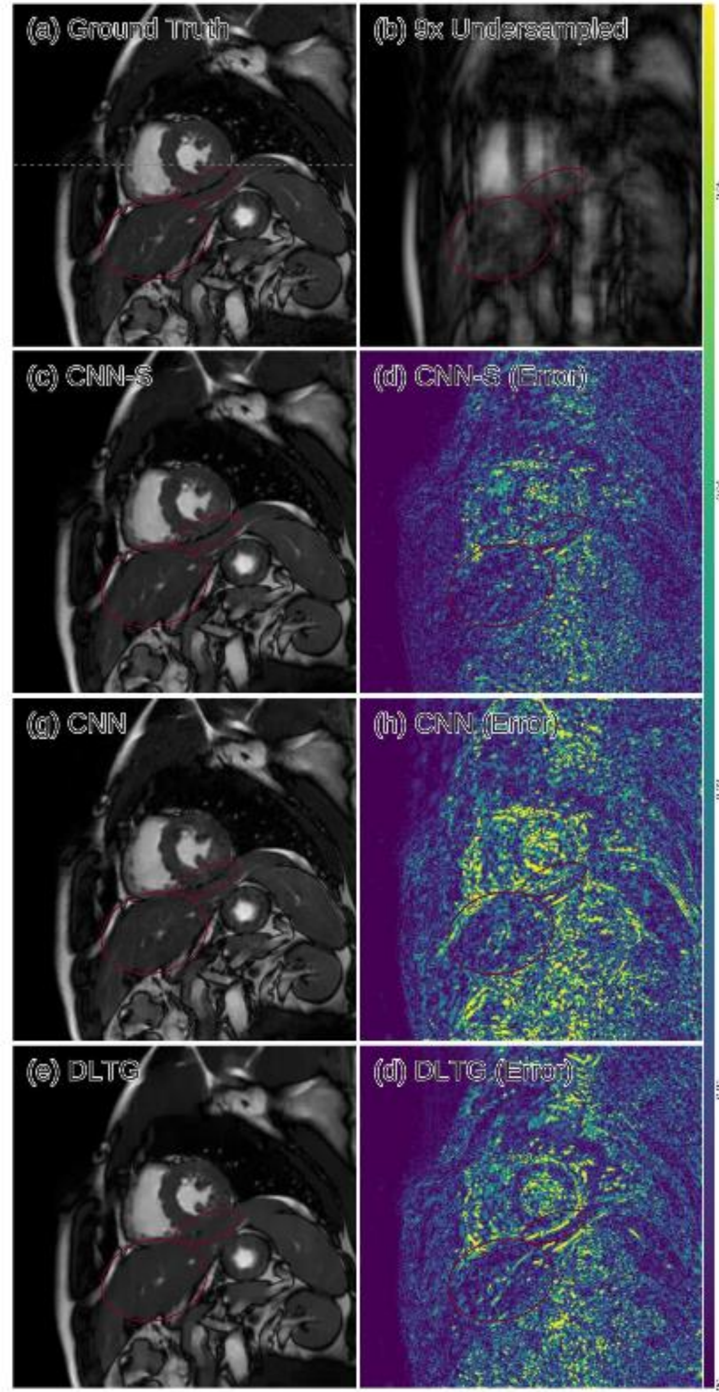

Deep Cascade CNNs

- [Schlemper et al. 2017]: Results
- Test error across 10 subjects:

Model	R=4 (dB)	R=8 (dB)
DLTG	27.5 (1.31)	22.6 (0.95)
CNN	31.0 (1.08)	25.2 (1.00)

Model	Time
DLTG	~6 hr (CPU)
CNN (2D)	0.69 s (GPU)
CNN (2D+t)	10 s (GPU)

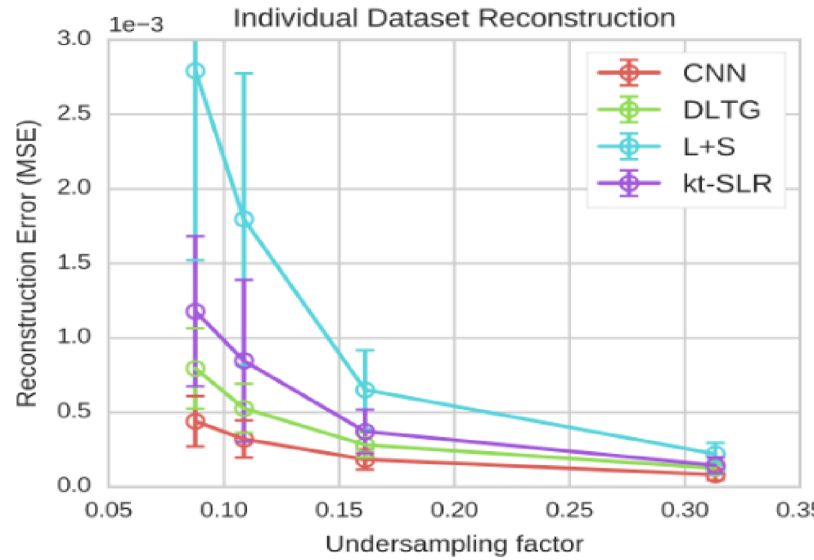

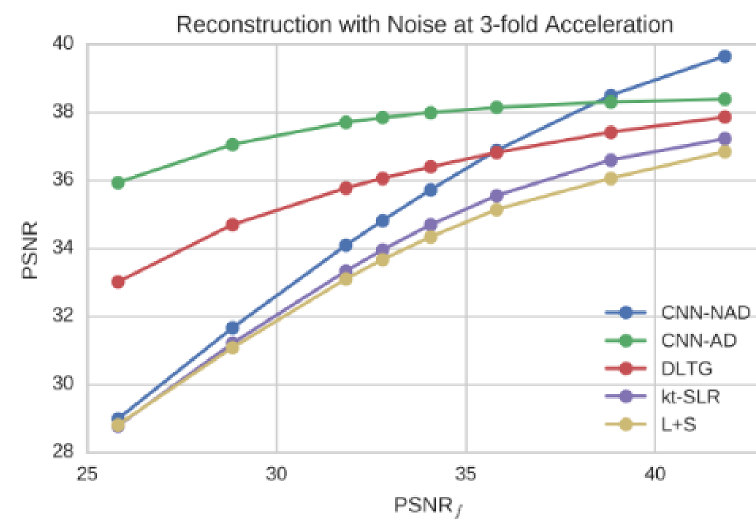

Couple Enhancement and Segmentation

- [Oktay et al. 2017]: Insert anatomical constrains into the enhancement problem.
  - Acquisition of cardiac MRI typically consists of 2D multi-scale data due to
    - Constraints on SNR
    - Breath-hold time
    - Total acquisition time
  - This leads to thick slice data (thickness 8-10 mm per slice)
  - Motion between slices can lead to artefacts

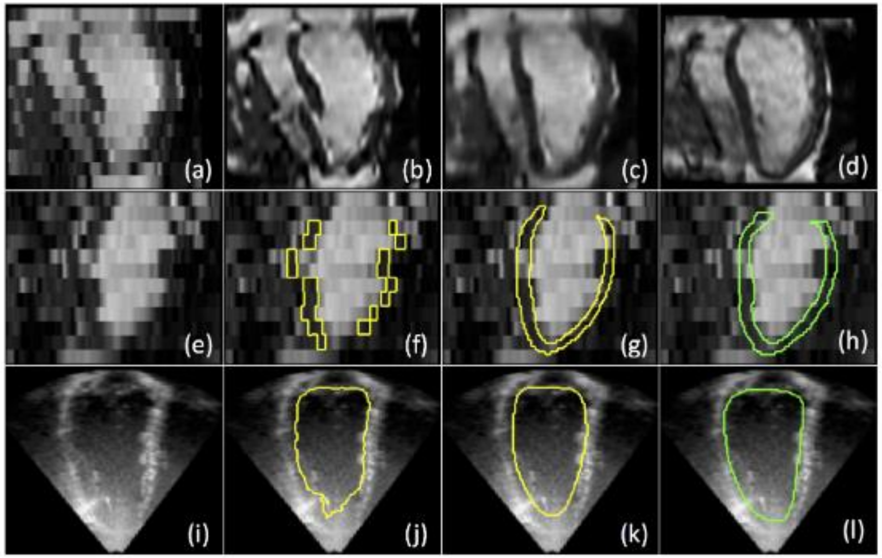

Couple Enhancement and Segmentation

- [Oktay et al. 2017]

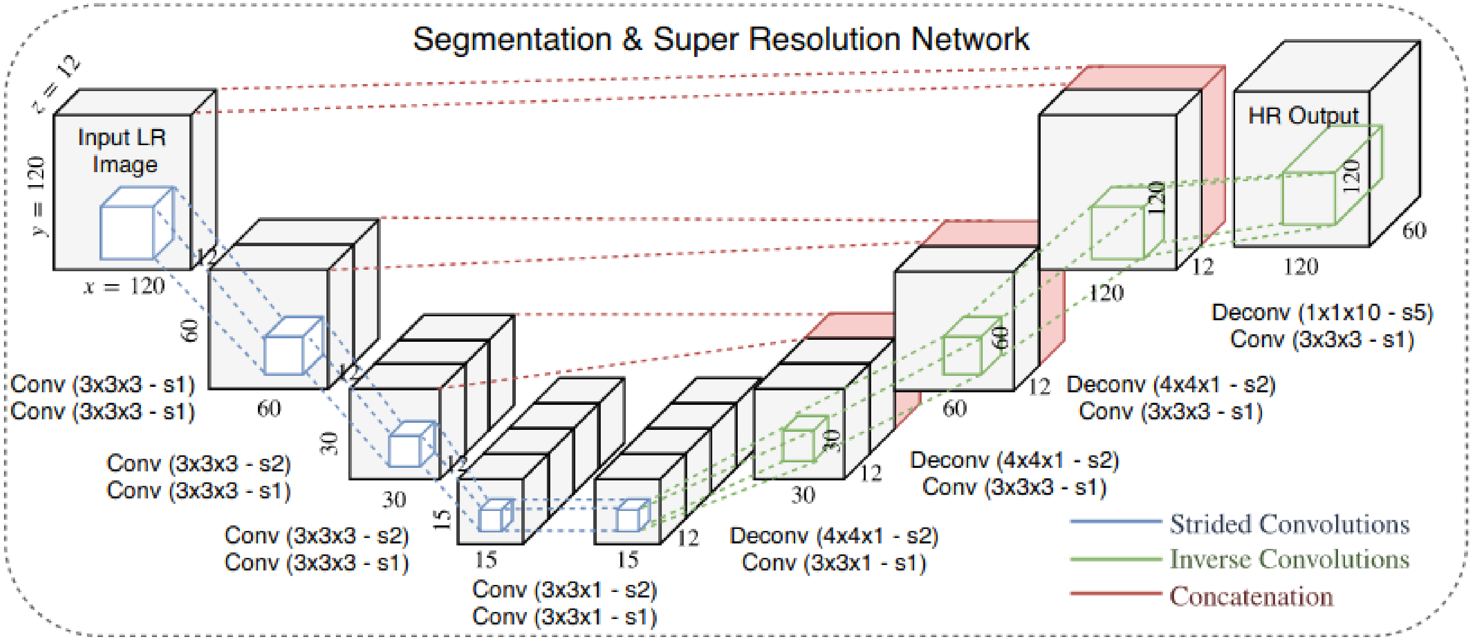

$$L_{h_e} = \| f(\phi(\boldsymbol{x}); \boldsymbol{\theta}_f) - f(\boldsymbol{y}; \boldsymbol{\theta}_f) \|_2^2 \qquad L_x = -\sum_{c=1}^{C} \sum_{i \in \mathcal{S}} \log \left(\frac{e^{f_{(c,i)}}}{\sum_j e^{f_{(j,i)}}} \right)$$

$$\min_{\boldsymbol{\theta}_s} \left(L_x \left(\phi(\boldsymbol{x}; \boldsymbol{\theta}_s), \boldsymbol{y} \right) + \lambda_1 \cdot L_{h_e} + \frac{\lambda_2}{2} ||\boldsymbol{w}||_2^2 \right)$$

Couple Enhancement and Segmentation

- [Oktay et al. 2017]

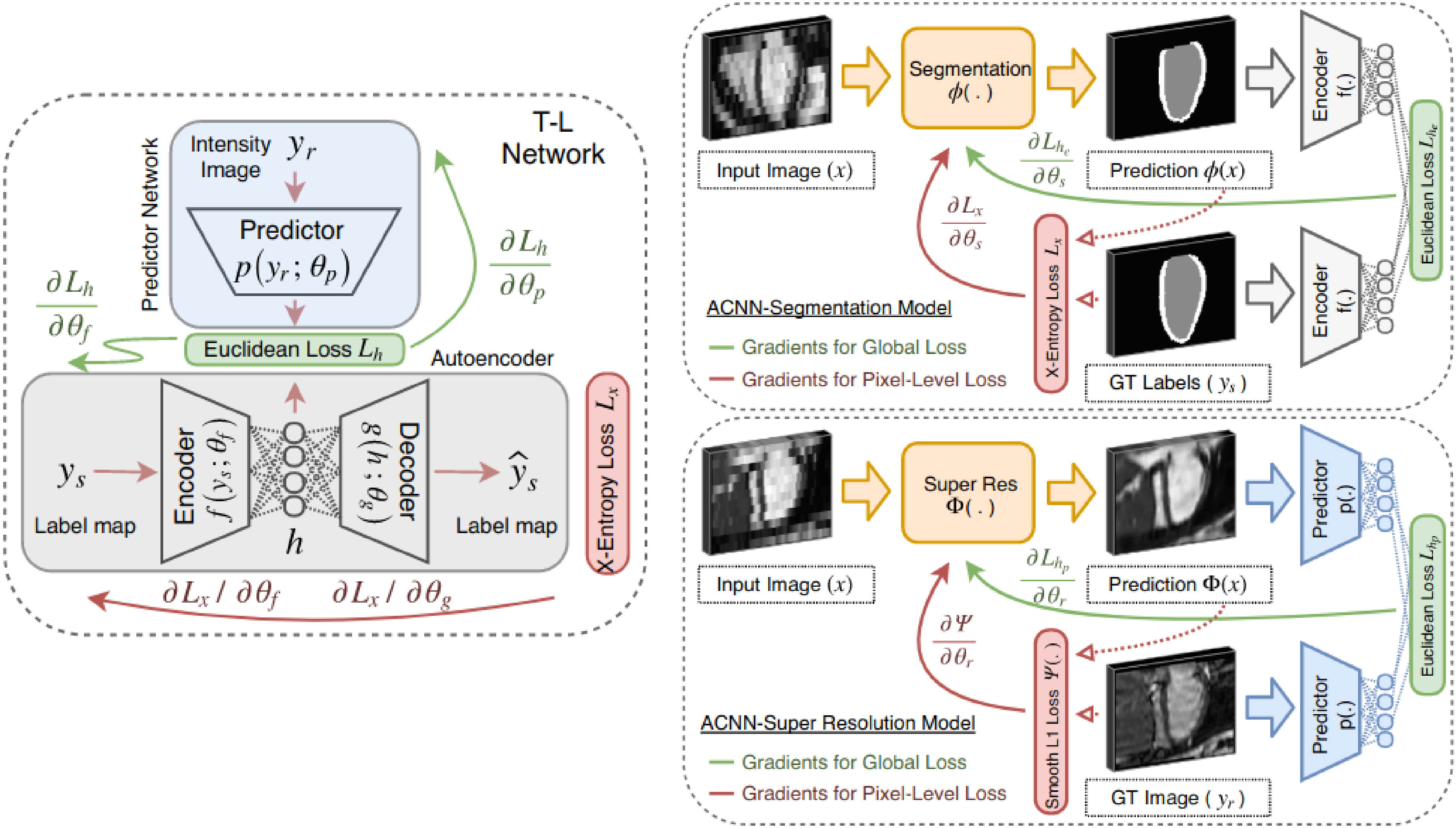

Couple Enhancement and Segmentation

- [Oktay et al. 2017]: Insert anatomical constrains into the enhancement problem.

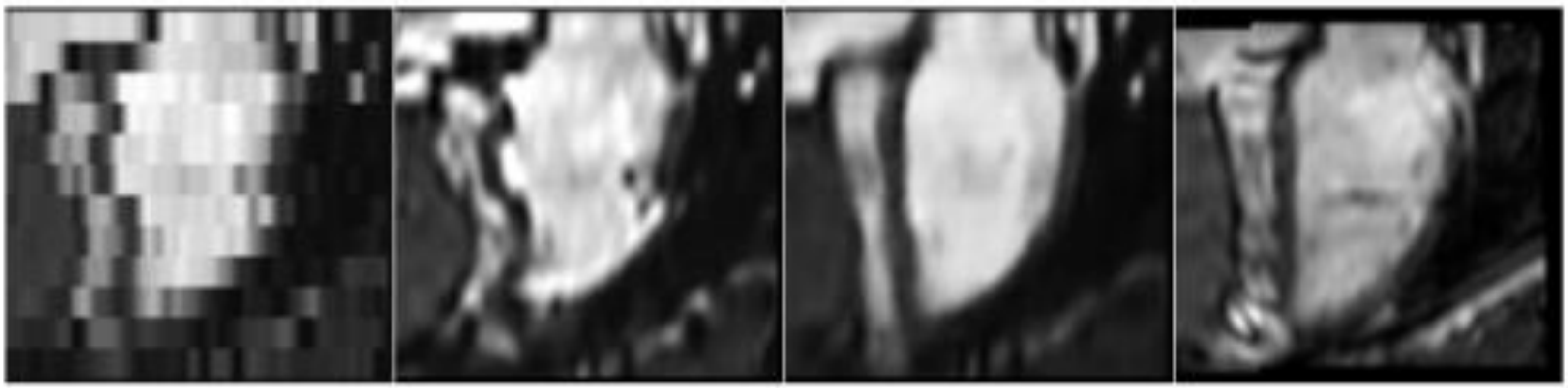

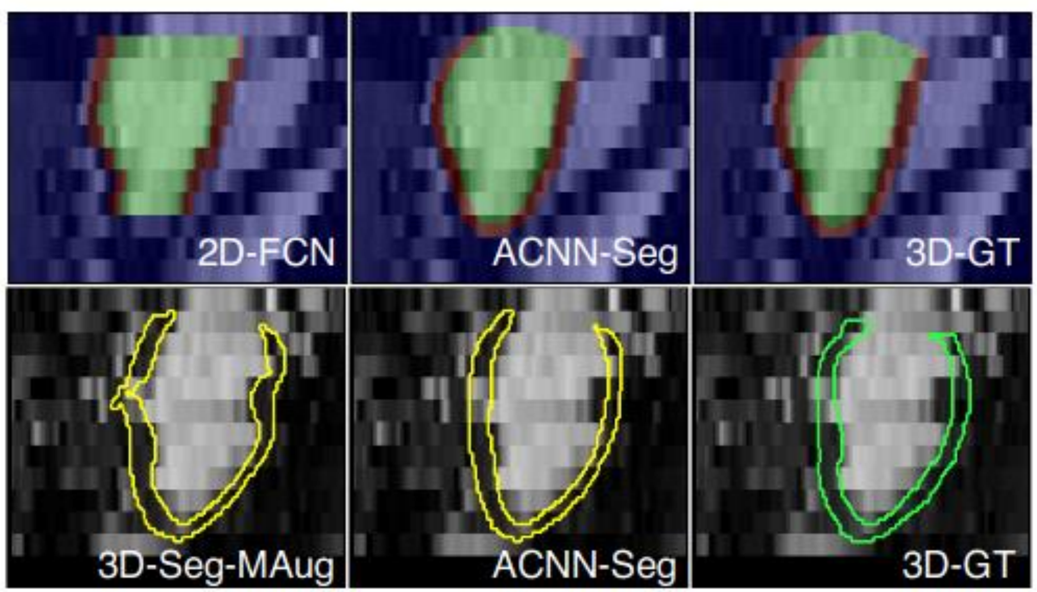

Couple Enhancement and Segmentation

- [Oktay et al. 2017]: Insert anatomical constrains into the enhancement problem.

	Endocardium			Myocardium			Capacity
	Mean Dist. (mm)	Hausdorff Dist. (mm)	Dice Score (%)	Mean Dist. (mm)	Hausdorff Dist. (mm)	Dice Score (%)	# Trainable Parameters
2D-FCN [44]	2.07±0.61	11.37±7.15	.908±.021	1.58±0.44	9.19±7.22	.727±.046	1.39×10^6
3D-Seg	1.77±0.84	10.28±8.25	.923±.019	1.48±0.51	10.15±10.58	.773±.038	1.60×10^6
3D-UNet [12]	1.66±0.74	9.94±9.22	.923±.019	1.45±0.47	9.81±11.77	.764±.045	1.64×10^6
AE-Seg [37]	1.75±0.58	8.42±3.64	.926±.019	1.51±0.29	8.52±2.72	.779±.033	1.68×10^6
3D-Seg-MAug	1.59±0.74	8.52±8.13	.928±.019	1.37±0.41	9.41±9.17	.785±.041	1.60×10^6
AE-Seg-M	1.59±0.48	**7.52±3.78**	.927±.017	1.32±0.26	**7.12±2.79**	.791±.036	1.91×10^6
ACNN-Seg	**1.37±0.42**	7.89±3.83	**.939±.017**	**1.14±0.22**	7.31±3.59	**.811±.027**	1.60×10^6
p-values	$p \ll 0.001$	$p \approx 0.890$	$p \ll 0.001$	$p \ll 0.001$	$p \approx 0.071$	$p \ll 0.001$	-

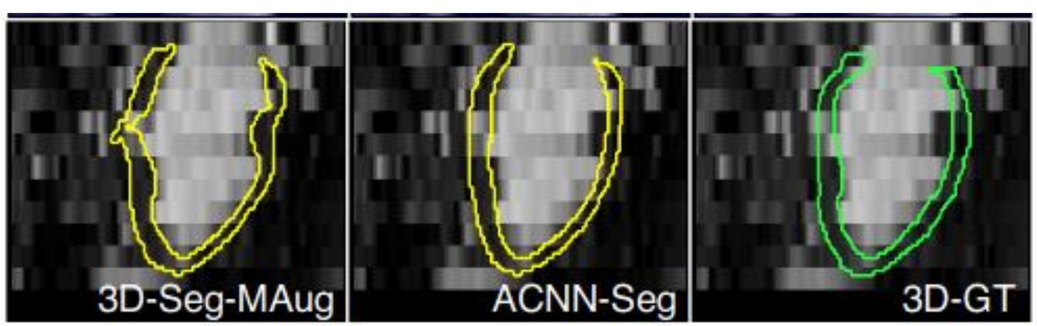

More Papers

Denoising on XRays

- [Sori et al. 2017] Design of a deep feed forward CNN model which directly approximate the noise from a noisy image. Residual learning is approximated, and batch normalization is also incorporated to boost model performance.

$$l(\lambda) = \frac{1}{2N} \sum_{k=1}^{N} \| \Re(z_k; \lambda) - (z_k - x_k) \|_F^2$$

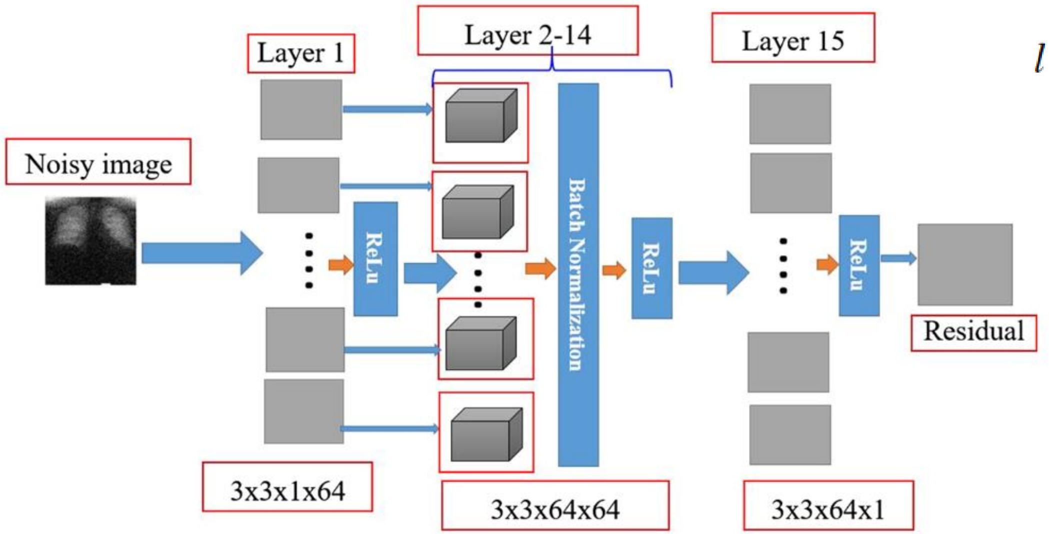

Fig. 1 Residual learning phase of the model for medical image denoising

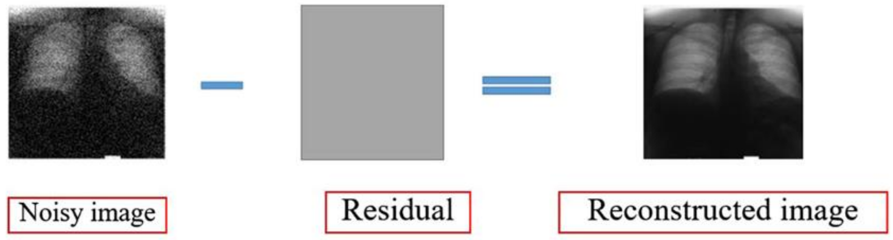

Denoising on XRays

- [Sori et al. 2017]

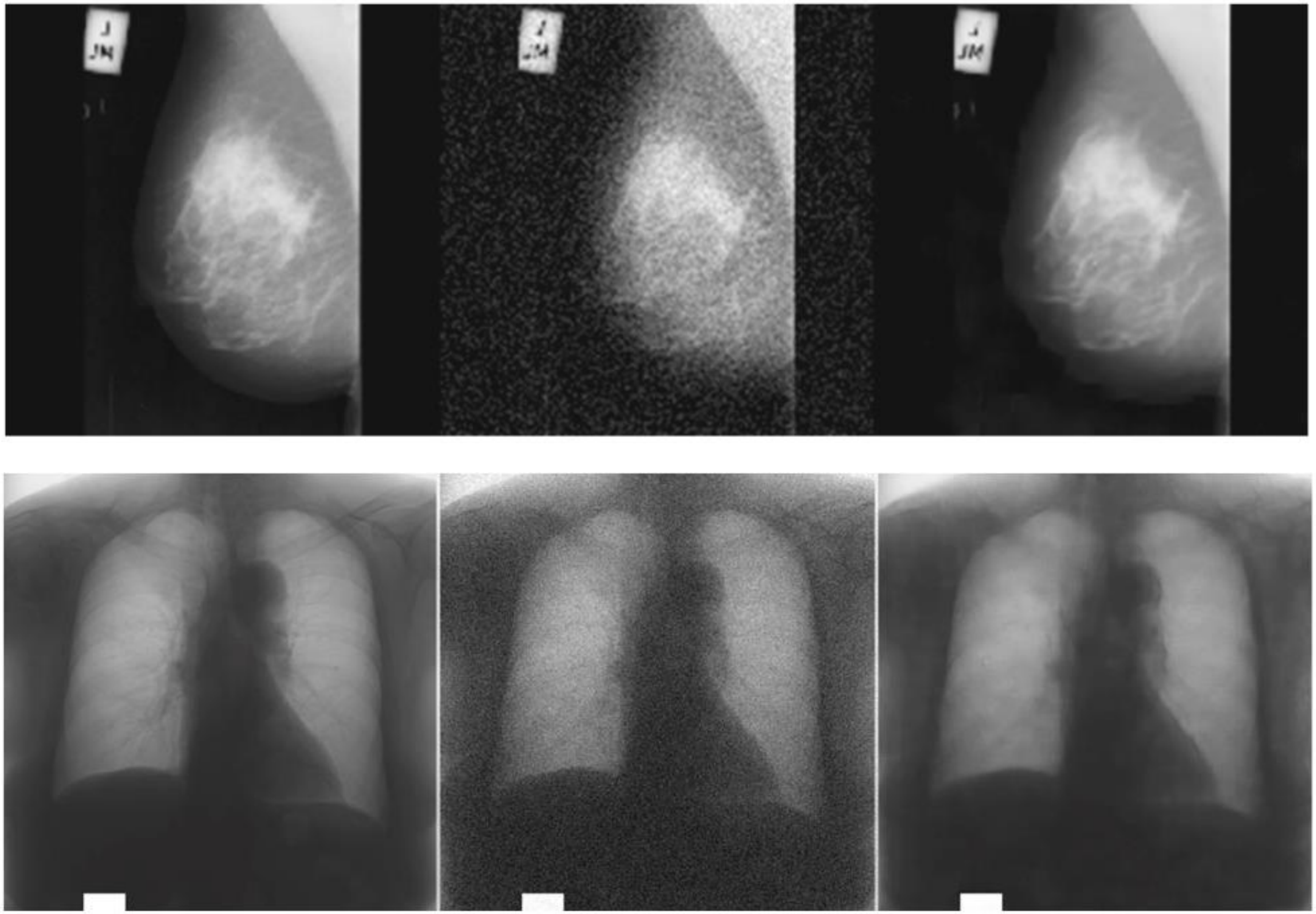

Denoising on XRays

- [Sori et al. 2017]

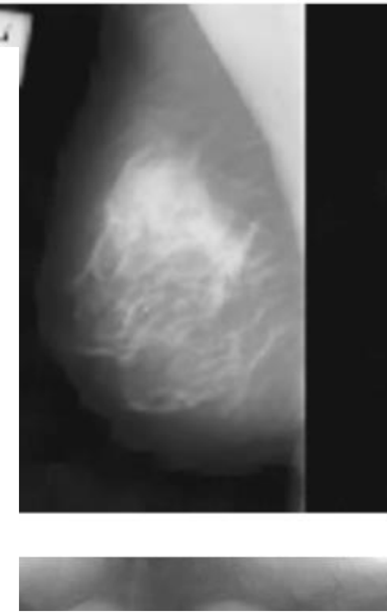

Noise level	Methods			
	Metrics	BM3D	DnCNN	Proposed
Model trained on i.s 180×180, i.s.s 547 and b.s 128				
15	PSNR	40.018	41.116	41.217
	SSIM	–	0.963	0.963
25	PSNR	37.265	38.871	38.882
	SSIM	–	0.949	0.959

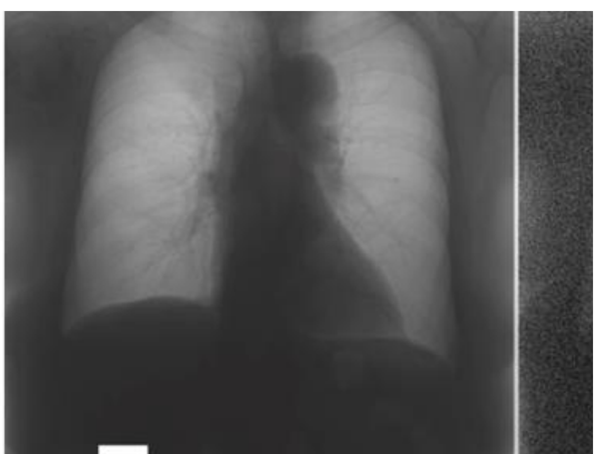

Noise level	Methods			
	Metrics	CNN DAE	DnCNN	Proposed
Model trained on i.s 64×64, i.s.s 235 and b.s 10				
15	PSNR	–	39.246	39.250
	SSIM	0.89	0.950	0.950
25	PSNR	–	36.696	36.70
	SSIM	0.89	0.932	0.932

Low Dose CT Image Denoising

- [Yang et al. 2018] Computed tomography (CT) is one of the most important modalities. Potential radiation rist to the patient since x-rays could cause generic damage
- Lower radiation increases noise and artifacts

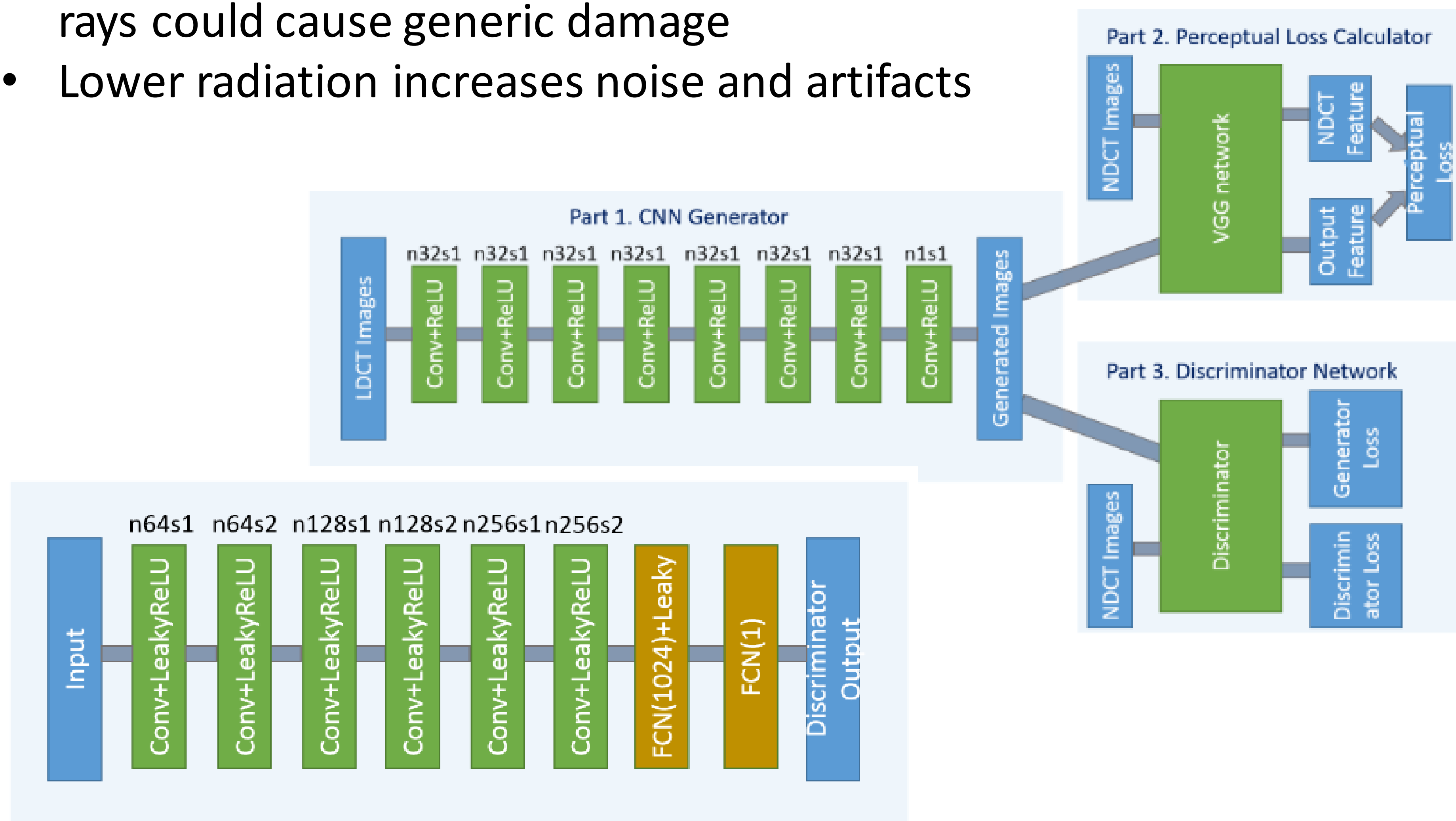

Low Dose CT Image Denoising

- [Yang et al. 2018]

	Fig. 5		Fig. 7	
	PSNR	SSIM	PSNR	SSIM
LDCT	19.7904	0.7496	18.4519	0.6471
CNN-MSE	24.4894	0.7966	23.2649	0.7022
WGAN-MSE	24.0637	0.8090	22.7255	0.7122
CNN-VGG	23.2322	0.7926	22.0950	0.6972
WGAN-VGG	23.3942	0.7923	22.1620	0.6949
WGAN	22.0168	0.7745	20.9051	0.6759
‘1 GAN	21.8676	0.7581	21.0042	0.6632
DictRecon	24.2516	0.8148	24.0992	0.7631

	Fig. 5		Fig. 7	
	Mean	SD	Mean	SD
NDCT	9	36	118	38
LDCT	11	74	118	66
CNN-MSE	12	18	120	15
WGAN-MSE	9	28	115	25
CNN-VGG	4	30	104	28
WGAN-VGG	9	31	111	29
WGAN	23	37	135	33
GAN	8	35	110	32
DictRecon	4	11	111	13

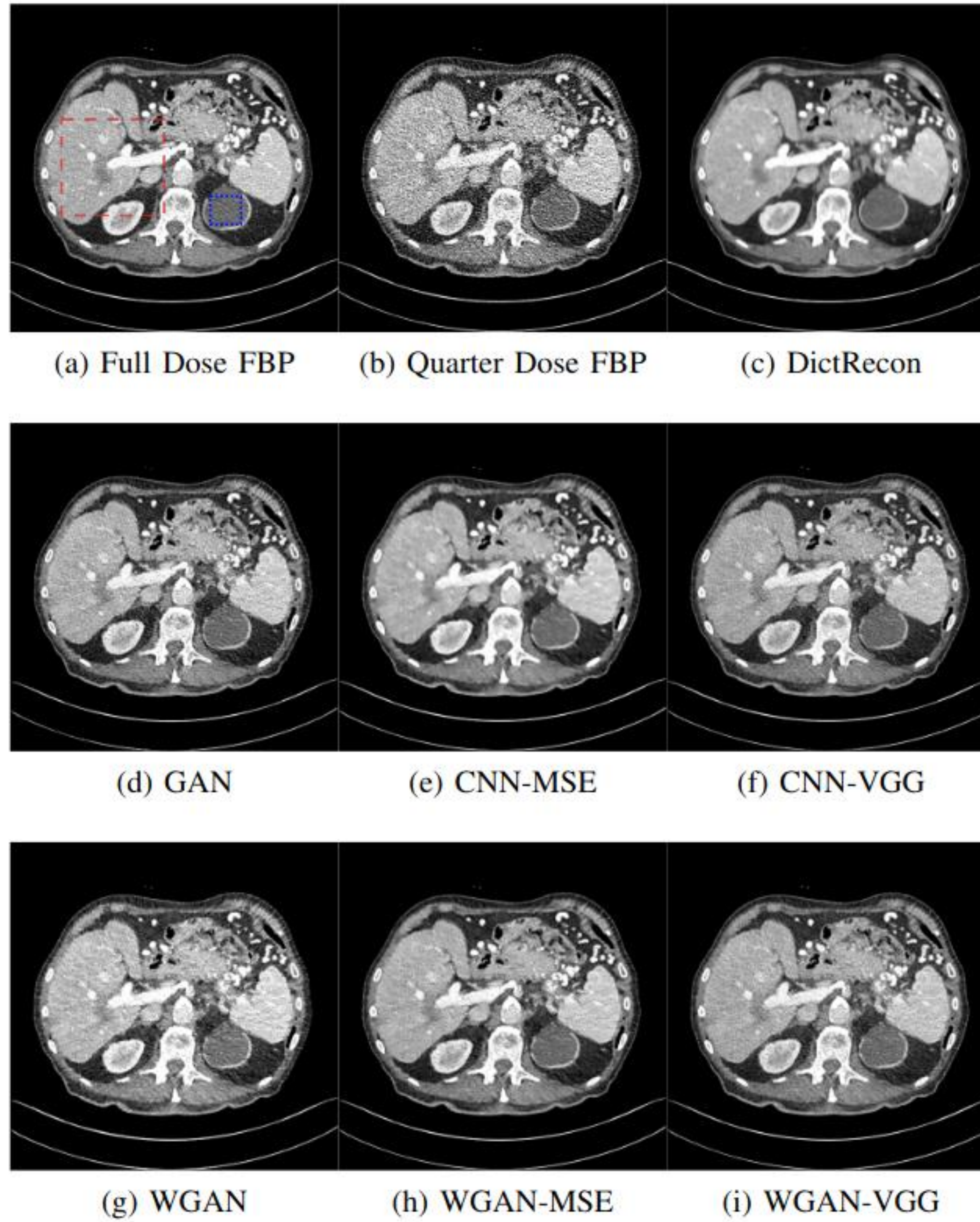

Low Dose CT Image Denoising

- [Yang et al. 2018]

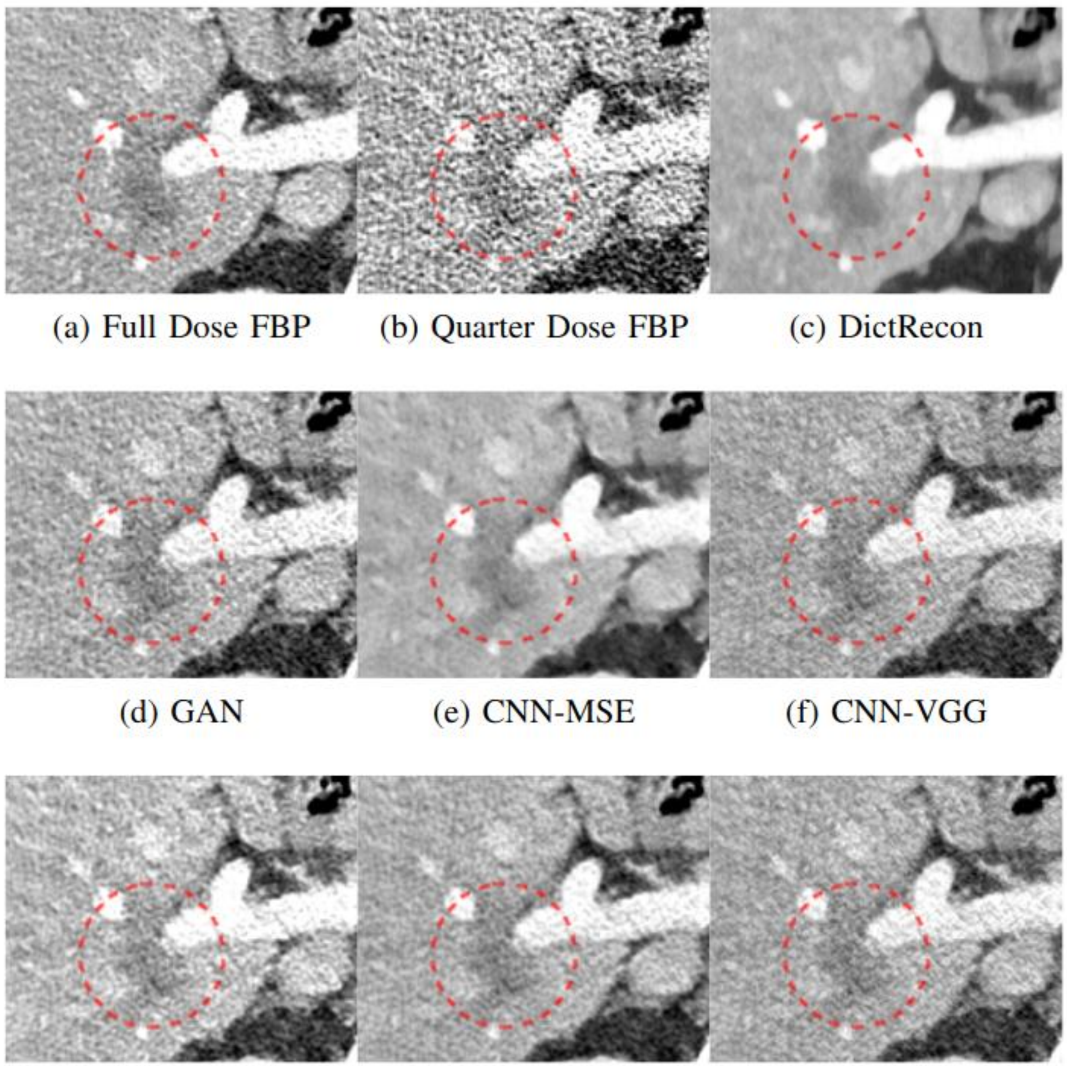

(a) Full Dose FBP (b) Quarter Dose FBP (c) DictRecon

(d) GAN (e) CNN-MSE (f) CNN-VGG

(g) WGAN (h) WGAN-MSE (i) WGAN-VGG

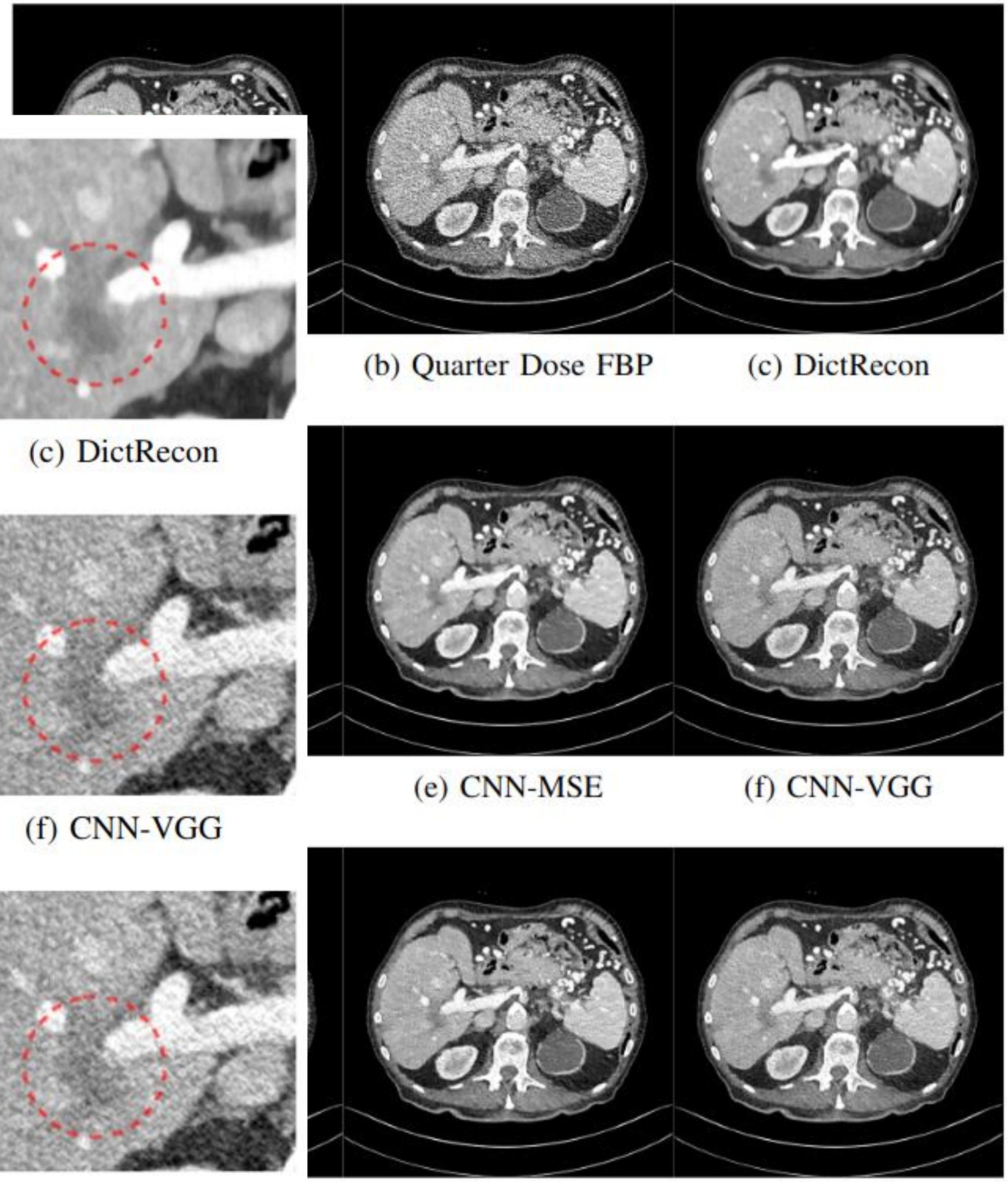

(b) Quarter Dose FBP (c) DictRecon

(e) CNN-MSE (f) CNN-VGG

(h) WGAN-MSE (i) WGAN-VGG

Learning Brain MRI Manifolds

- [Bernudez et al. 2018] Unsupervised synthesis of T1-weighted brain MRI using a Generative Adversarial Network (GAN)

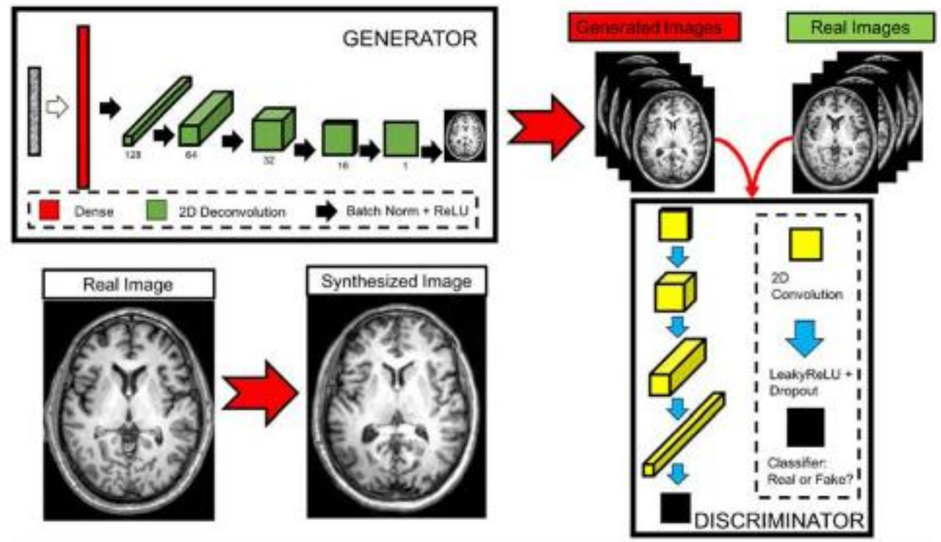

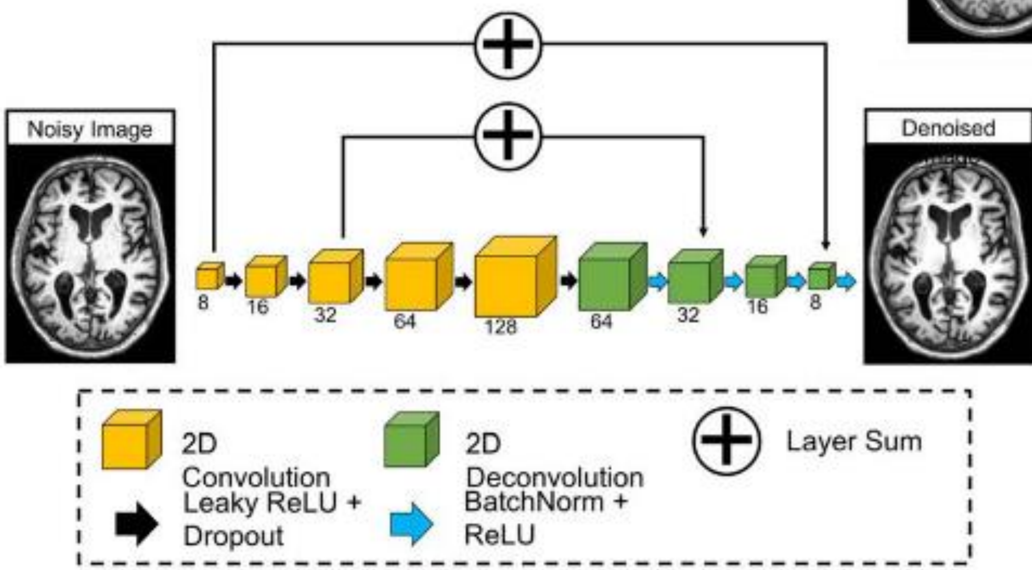

Learning Brain MRI Manifolds

- [Bernudez et al. 2018] Unsupervised synthesis of T1-weighted brain MRI using a Generative Adversarial Network (GAN)

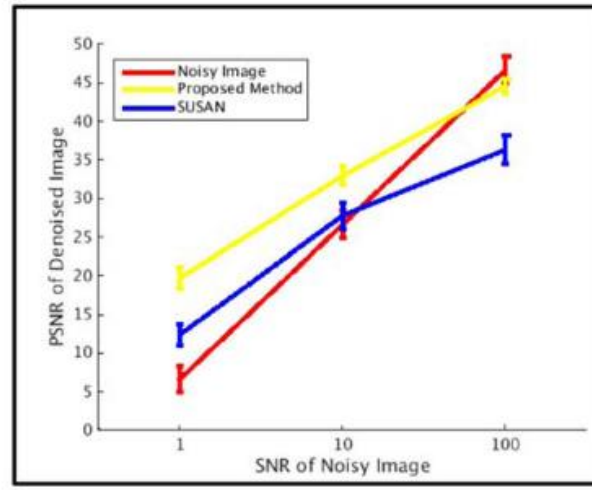

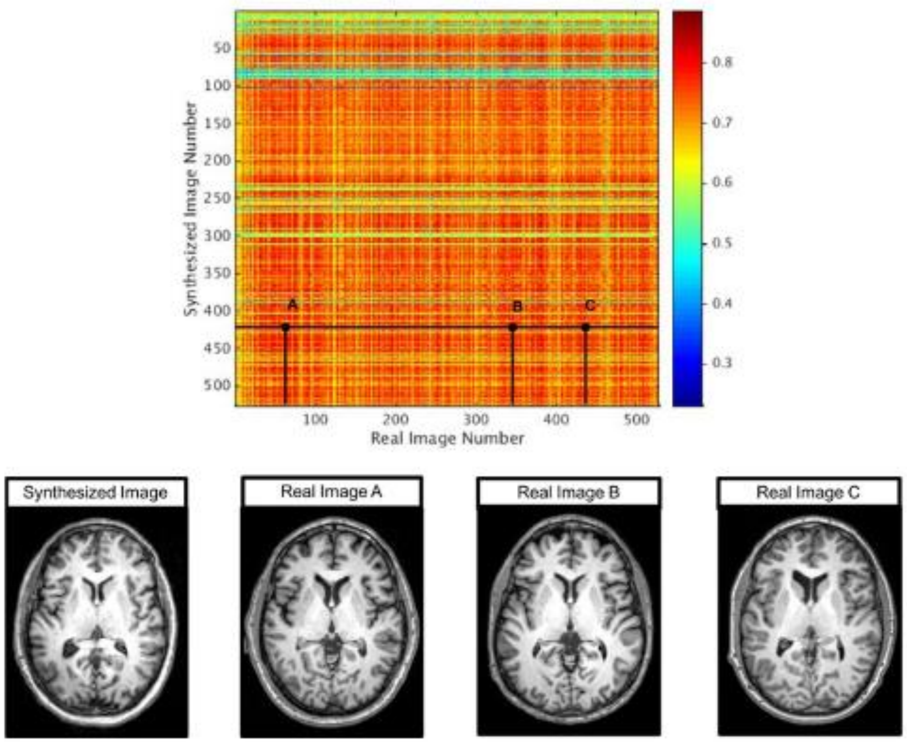

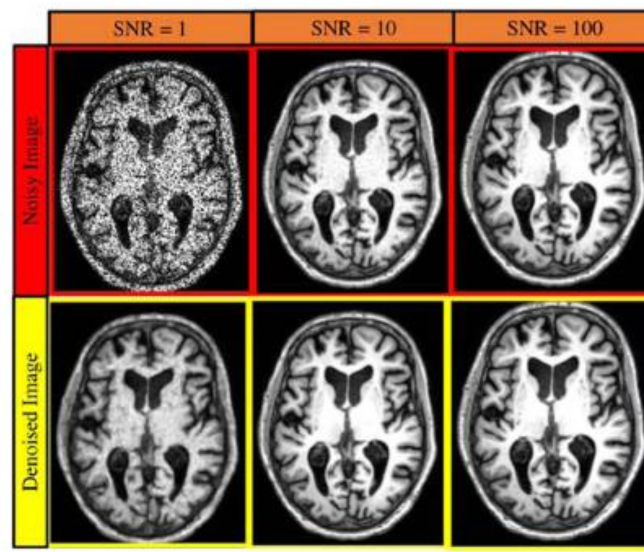

A CNN to filter artifacts

- [Gurbani et al. 2017] A deep learning model was developed that was capable of identifying andfiltering out poor quality spectra. The core of the model used a tiled CNN that analyzed frequency-domain spectra to detect artifacts.
- The Cho/NAA ratio is widely used for depiction of tumor volumes and infil-tration as a result of increased contrast caused by the opposite changes of these metabolites in the tumor.

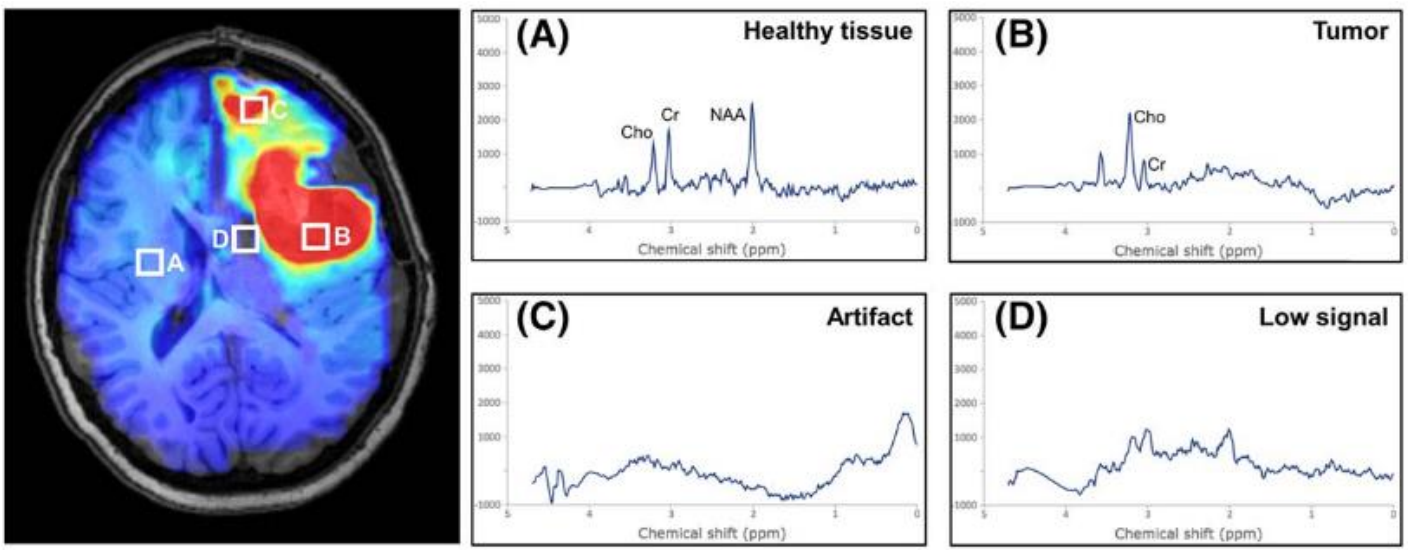

FIGURE 1 Artifacts in MRSI arise for several reasons and can lead to false interpretation of pathology. A, Healthy tissue shows a relatively low Cho/NAA ratio. B, Tumor shows an elevated ratio, appearing as hyperintense on a Cho/NAA map. Artifacts can arise in tissue boundaries and in areas with poor lipid or water suppression, and can result in either hyperintense lesions (C) or dropout of signal (D)

A CNN to filter artifacts

- [Gurbani et al. 2017] A deep learning model was developed that was capable of identifying and filtering out poor quality spectra. The core of the model used a tiled CNN that analyzed frequency-domain spectra to detect artifacts.

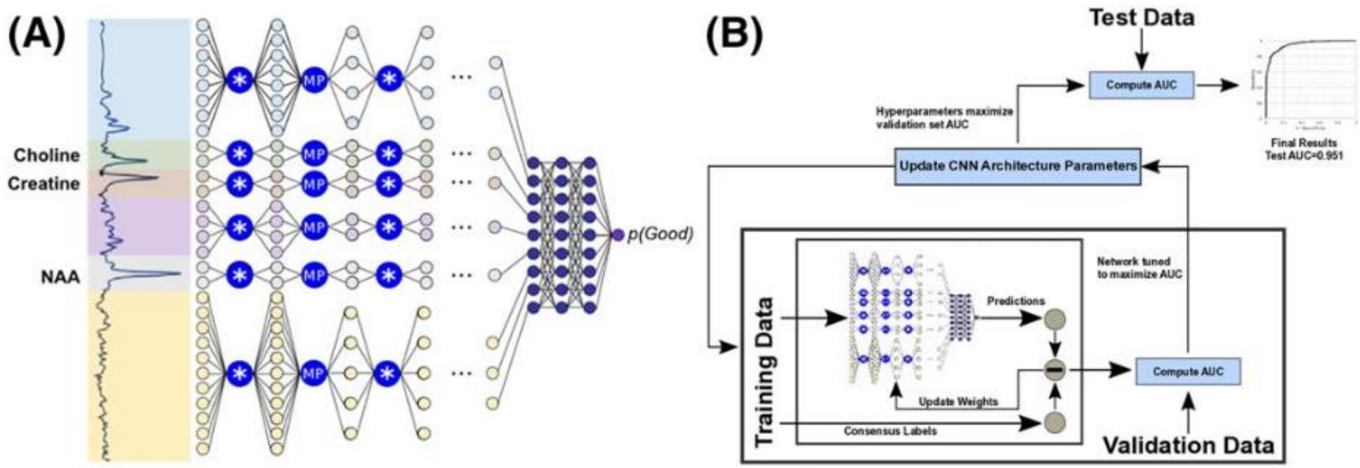

FIGURE 3 A, High-level overview of the convolutional neural network (CNN) for spectral quality analysis. Input spectra are split into 6 tiles and passed through a series of convolution (*) and max-pooling (MP) layers, then concatenated and passed through fully connected layers to generate a scalar output of spectral quality. B, Bayesian optimization is used to iteratively optimize architecture hyperparameters. AUC, area under the curve

A CNN to filter artifacts

- [Gurbani et al. 2017] A deep learning model was developed that was capable of identifying and filtering out poor quality spectra. The core of the model used a tiled CNN that analyzed frequency-domain spectra to detect artifacts.

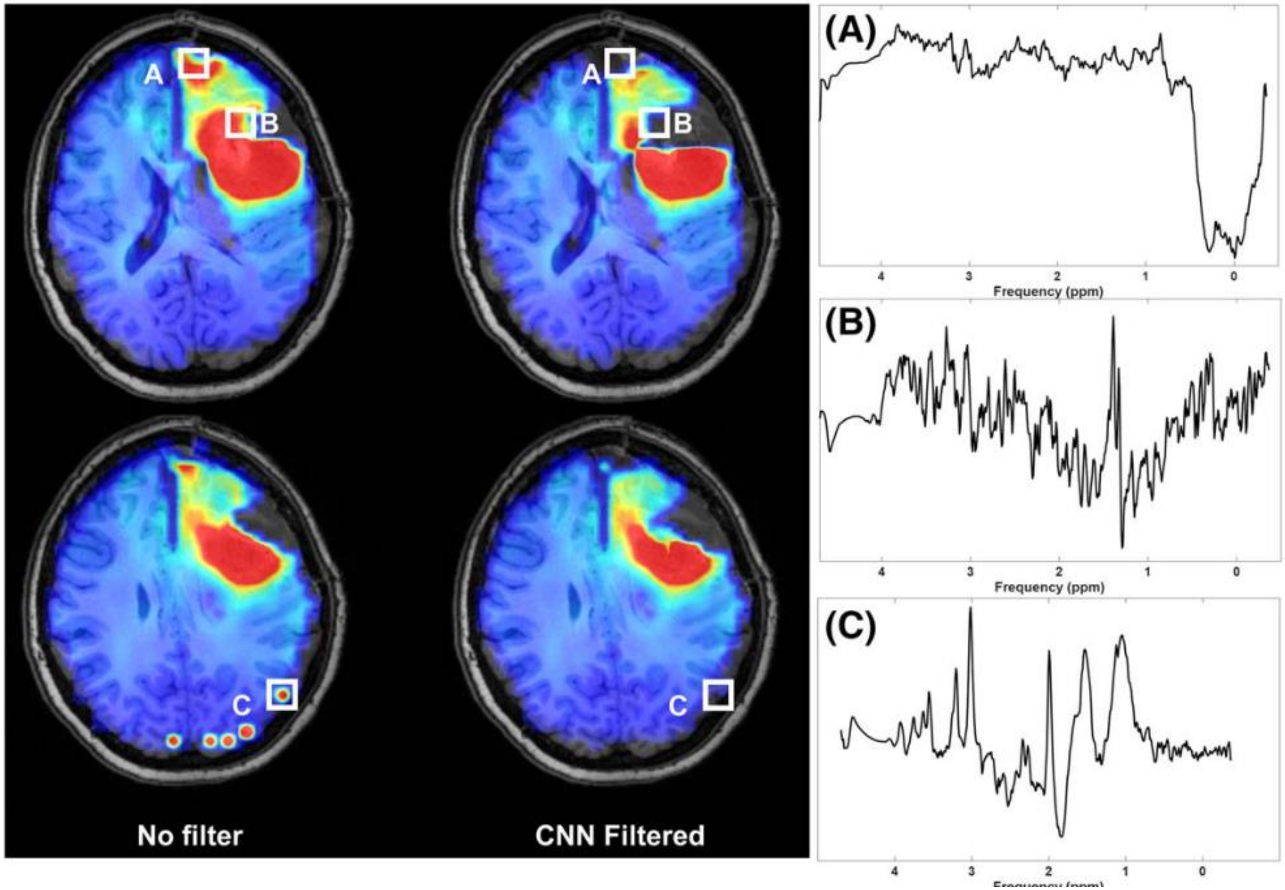

Unsupervised denoising

- [Zhussip et al. 2019] Propose a novel method based on two theories: denoiser-approximate message passing (D-AMP) and Stein's unbiased risk estimator (SURE).
- D-AMP Algorithm

$$\min_{\boldsymbol{x}} \|\boldsymbol{y} - \boldsymbol{A}\boldsymbol{x}\|_2^2 \quad \text{subject to} \quad \boldsymbol{x} \in C$$

Where C is the set of natural images.

The solution relys on approximate message passing (AMP) theory

The D-AMP algorithm traditionally uses conventional state-of-the-art denoisers. Recently it is applied also with CNNs. These denoisers can be defined as: $\boldsymbol{D}_{\boldsymbol{w}(\hat{\sigma}_t)}(\cdot)$

Unsupervised denoising

- [Zhussip et al. 2019] Propose a novel method based on two theories: denoiser-approximate message passing (D-AMP) and Stein's unbiased risk estimator (SURE).
- Stein's unbiased risk estimator (SURE)

$$\frac{1}{K}\sum_{j=1}^{K}\|\boldsymbol{D}_{\boldsymbol{w}(\sigma)}(\boldsymbol{z}^{(j)}) - \boldsymbol{x}^{(j)}\|^2$$

Between the output of the denoiser and the ground truth image. Recently [Soltanayev et al., 2018] has been proposed an approximation of this formulation following Monte-Calro Stein's unbiased rish estimator (MC-SURE)

$$\frac{1}{K}\sum_{j=1}^{K}\|\boldsymbol{z}^{(j)} - \boldsymbol{D}_{\boldsymbol{w}(\sigma)}(\boldsymbol{z}^{(j)})\|^2 - N\sigma^2 +$$
$$\frac{2\sigma^2\tilde{\boldsymbol{n}}'}{\epsilon}\left(\boldsymbol{D}_{\boldsymbol{w}(\sigma)}(\boldsymbol{z}^{(j)} + \epsilon\tilde{\boldsymbol{n}}) - \boldsymbol{D}_{\boldsymbol{w}(\sigma)}(\boldsymbol{z}^{(j)})\right).$$

Unsupervised denoising

- [Zhussip et al. 2019] Results:

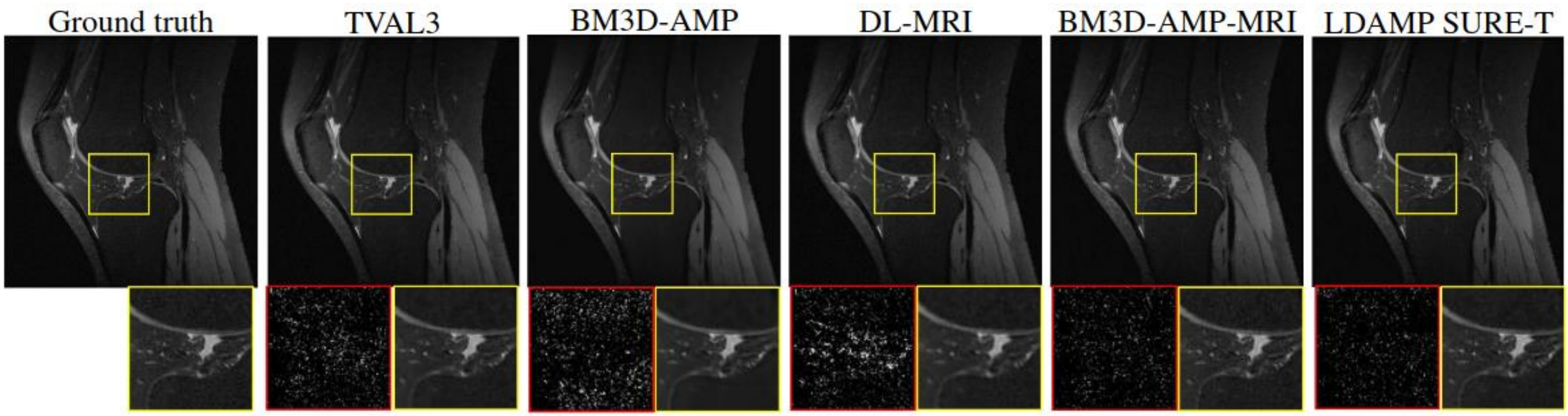

(a) PSNR (b) 37.44 dB (c) 36.54 dB (d) 36.76 dB (e) 37.85 dB (f) **38.22 dB**

Method	Training Time	$\frac{M}{N} = 5\%$		$\frac{M}{N} = 15\%$		$\frac{M}{N} = 25\%$	
		PSNR	Time	PSNR	Time	PSNR	Time
TVAL3	N/A	20.46	9.71	24.14	22.96	26.77	34.87
NLR-CS	N/A	**21.88**	128.73	27.58	312.92	31.20	452.23
BM3D-AMP	N/A	21.40	25.98	26.74	24.21	30.10	23.08
LDAMP BM3D	10.90 hrs	21.41	8.98	27.54	3.94	31.20	2.89
LDAMP BM3D-T	14.30 hrs	21.42	8.98	27.61	3.94	31.32	2.89
LDAMP SURE	15.05 hrs	21.44	8.98	27.65	3.94	31.46	2.89
LDAMP SURE-T	17.97 hrs	21.68	**8.98**	**27.84**	**3.94**	**31.66**	**2.89**
LDAMP MSE	10.17 hrs	22.07	8.98	27.78	3.94	31.65	2.89

Conclusions

- Image reconstruction and denoising is very important for medical imaging.
- Variety of metrics can be used for the evaluation of the denoised image.
- Very important to find formulations that can be verified from the physics or well established theories.
- Unsupervised methods and adversarial networks will play a significant role in the future. Really active research area.
- Challenges
    - Learning the right features
    - Detecting when it goes wrong
    - Going beyond human-level performance

Lab Session!

- Denoising of Mammograms
  - Dilated filters

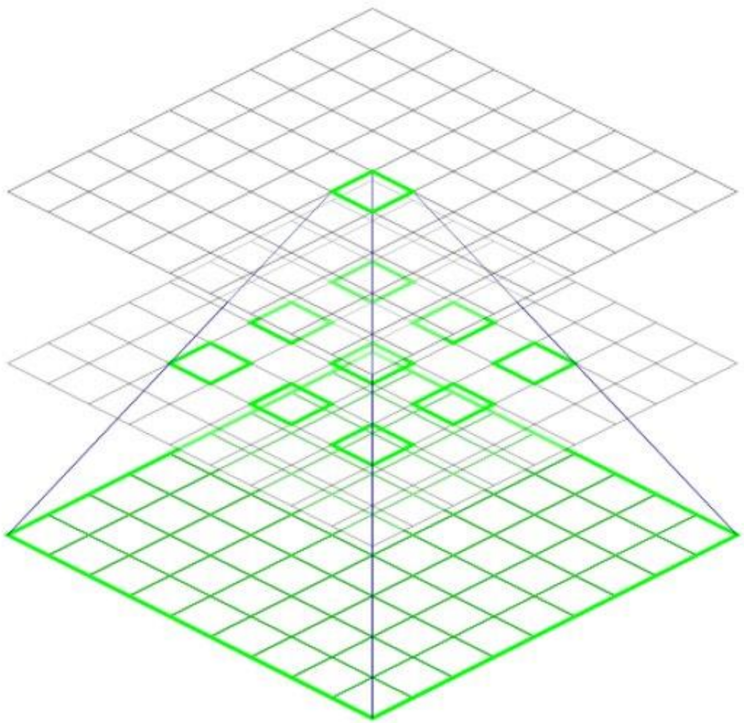

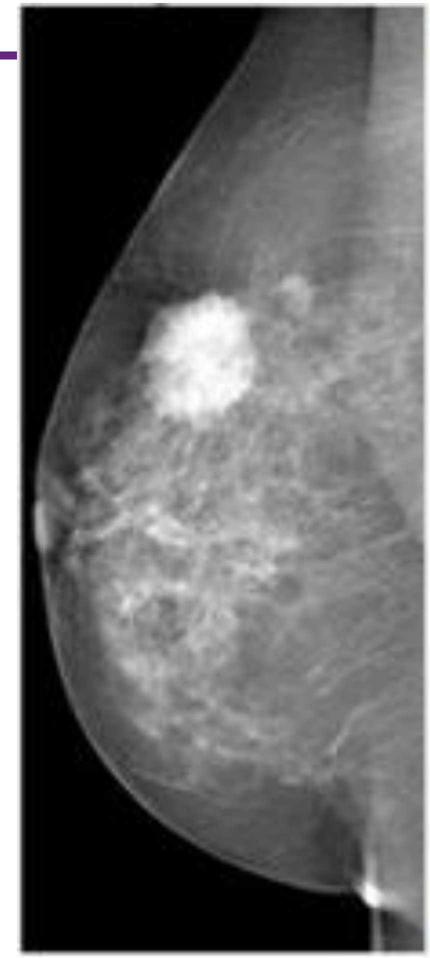

jupyter

PyTorch

TorchVision

Facebook Open Source

Deep learning for medical imaging

Olivier Colliot, PhD
Research Director at CNRS
Co-Head of the ARAMIS Lab – www.aramislab.fr
PRAIRIE – Paris Artificial Intelligence Research Institute

Maria Vakalopoulou, PhD
Assistant Professor at CentraleSupelec
Mathematics and Informatics (MICS)
Office: Bouygues Building Sb.132

Master 2 - MVA

Course website: http://www.aramislab.fr/teaching/DLMI-2019-2020/
Piazza (for registered students):
https://piazza.com/centralesupelec/spring2020/mvadlmi/